

Spin-charge-separated quasiparticles in one-dimensional quantum fluids

F. H. L. Essler,¹ R. G. Pereira,² and I. Schneider³

¹*The Rudolf Peierls Centre for Theoretical Physics, Oxford University, Oxford OX1 3NP, United Kingdom*

²*Instituto de Física de São Carlos, Universidade de São Paulo, C.P. 369, São Carlos, SP, 13560-970, Brazil*

³*Department of Physics and Research Center OPTIMAS, University of Kaiserslautern, D-67663 Kaiserslautern, Germany*

(Received 30 April 2015; published 24 June 2015)

We revisit the problem of dynamical response in spin-charge separated one-dimensional quantum fluids. In the framework of Luttinger liquid theory, the dynamical response is formulated in terms of noninteracting bosonic collective excitations carrying either charge or spin. We argue that, as a result of spectral nonlinearity, long-lived excitations are best understood in terms of generally strongly interacting fermionic holons and spinons. This has far reaching ramifications for the construction of mobile impurity models used to determine threshold singularities in response functions. We formulate and solve the appropriate mobile impurity model describing the spinon threshold in the single-particle Green's function. Our formulation further raises the question whether it is possible to realize a model of noninteracting fermionic holons and spinons in microscopic lattice models of interacting spinful fermions. We investigate this issue in some detail by means of density matrix renormalization group (DMRG) computations.

DOI: [10.1103/PhysRevB.91.245150](https://doi.org/10.1103/PhysRevB.91.245150)

PACS number(s): 71.10.Pm, 71.10.Fd

I. INTRODUCTION

Understanding the essential features of a quantum many-body system usually entails finding a simple explanation of its low-energy spectrum in terms of weakly interacting, long-lived quasiparticles. For example, in Landau's Fermi liquid theory the quasiparticles are fermions carrying the same quantum numbers as an electron, namely, charge e and spin $1/2$. However, it is well established that the long-lived excitations in strongly correlated systems may carry only a fraction of the quantum numbers of the elementary constituents. In fact, fractionalization is often invoked as a route towards exotic phases of matter such as spin liquids or high-temperature superconductors [1].

Perhaps the most prominent example of fractionalization is spin-charge separation in one-dimensional (1D) quantum fluids known as Luttinger liquids [2]. The hallmark of these theories is a low-energy spectrum described by two decoupled free bosonic fields associated with collective spin and charge degrees of freedom, respectively. On the experimental side, the most direct evidence for spin-charge separation involves the observation of multiple peaks associated with spin and charge collective modes in dynamical response functions at fairly high energies [3–6], beyond the regime where Luttinger liquid theory is applicable. Spin-charge separation is known to persist at high energies for integrable theories such as the 1D Hubbard [7–16] and $1/r^2t$ - J [17,18] models. In these cases, any eigenstate with a finite energy in the thermodynamic limit can be classified in terms of elementary excitations called holons (which carry charge e and spin 0) and spinons (which carry charge 0 and spin $1/2$), along with their bound states. A convenient way for describing such excitations as well as their scattering is to define the corresponding creation and annihilation operators $Z_a^\dagger(\theta)$ and $Z_a(\theta)$, where a labels the different types of elementary excitations and θ is a variable that parameterizes the momentum $p_a(\theta)$ (the form of this function depends on the particular model under consideration). As a consequence of integrability, creation and annihilation operators fulfill the Faddeev-Zamolodchikov

algebra [19,20]:

$$\begin{aligned} Z_a(\theta_1)Z_b(\theta_2) &= S_{ab}^{cd}(\theta_1, \theta_2)Z_d(\theta_2)Z_c(\theta_1), \\ Z_a(\theta_1)Z_b^\dagger(\theta_2) &= 2\pi\delta(\theta_1 - \theta_2)\delta_{a,b} \\ &\quad + S_{bc}^{da}(\theta_2, \theta_1)Z_d^\dagger(\theta_2)Z_c(\theta_1). \end{aligned} \quad (1)$$

Here, $S_{ab}^{cd}(\theta_1, \theta_2)$ is the purely elastic two-particle S matrix. The corresponding elementary excitations are infinitely long lived, but generally strongly interacting, as can be seen from their scattering matrices [8–10]. Moreover, their quantum numbers, e.g., charge 0 and spin $1/2$ for spinons in the Hubbard model, differ from those of the collective bosonic spin modes in the Luttinger liquid description. It is natural to assume that breaking integrability slightly will not generically lead to a qualitative change in the nature of elementary holon and spinon excitations, but merely render the lifetimes finite.

How to reconcile this picture emerging from the exact solution with Luttinger liquid theory? In the latter, the nature of elementary excitations is obscured by the fact that, due to the linear dispersion approximation, the spectrum is highly degenerate and allows for many interpretations, which ultimately all give the same results for physical observables. Examples are chiral Luttinger liquid descriptions of quantum Hall edges [21] and the low-energy excitations of the Hubbard model. The latter can be understood both in terms of interacting, fermionic holons and spinons [7,22–24], and in terms of noninteracting bosons associated with collective spin and charge degrees of freedom [25–27].

Going beyond the linear dispersion approximation is expected to remove ambiguities in the quasiparticle description of the spectrum: there will be a particular choice that maximizes the lifetimes of elementary excitations. In integrable models such as the Hubbard chain, these lifetimes are infinite.

Over the last decade, it has been established in a series of works that going beyond the linear dispersion approximation is essential for correctly describing the dynamics of one-dimensional models with gapless excitations [28–56]. This has resulted in the so-called “nonlinear Luttinger liquid” (nLL)

approach to gapless 1D quantum liquids; see Refs. [46,54] for recent reviews. The basic reason for the failure of linear Luttinger liquid theory is that at finite energies the running coupling constants of irrelevant perturbations such as band curvature terms are in fact different from zero. Taking them into account in perturbation theory leads to infrared singularities. These need to be resummed to all orders in the coupling constants, which gives rise to new, momentum-dependent exponents in response functions.

A key ingredient of the nLL method is the identification of quasiparticles describing excited states both at high and at low energies. This is straightforward for spinless fermions, because the quasiparticles are adiabatically connected to free fermions [45]. The spinful case is considerably more involved due to the onset of spin-charge separation for arbitrarily weak interactions and the concomitant qualitative change in the nature of the elementary excitations compared to the noninteracting limit. It was realized in Refs. [49–52] that in many important cases exact results can be obtained by using a phenomenological model of weakly interacting fermionic holons and spinons, whose dispersions delineate the edges of the support of the dynamical response function under consideration. By construction, these excitations are different from the true elementary excitations in the Hubbard model. In particular, they carry different spin and charge quantum numbers. It is then an obvious but crucial question how to reconcile this approach with the exact solution of integrable models like the Hubbard chain.

In this work, we develop a new approach to deriving mobile impurity models for studying dynamical correlations in gapless models of spinful fermions. We first carry out a direct construction of the “physical” holon and spinon fields in the limit of weak electron-electron interactions. This results in a representation of spinful nonlinear Luttinger liquids in terms of strongly interacting holons and spinons, which is in direct accord with known results obtained in integrable cases. Recalling that the spinless fermion case was best understood by considering weak interactions, we address the construction of a microscopic model of interacting electrons giving rise to a theory of *noninteracting* fermionic holons and spinons at low energies, but in presence of spectral nonlinearities. We then derive mobile impurity models to analyze dynamical response functions in our formulation. We demonstrate explicitly how to recover results obtained previously by means of the approach of Refs. [51,52]. Finally, we address the question how to realize a lattice model of interacting electrons that gives rise to noninteracting holons and spinons at low energies.

II. SPINLESS FERMIONS

Before we approach the problem of defining quasiparticles for spin-1/2 fermions, it is instructive to review the case of spinless fermions. For concreteness, consider the simplest lattice model of interacting spinless fermions:

$$H = -t \sum_{j=1}^L (c_j^\dagger c_{j+1} + \text{H.c.}) + V \sum_j n_j n_{j+1}. \quad (2)$$

Here, c_j is the annihilation operator for a fermion at site j , $n_j = c_j^\dagger c_j$ is the number operator, t is the hopping parameter,

and V is the nearest-neighbor interaction strength. This model has a $U(1)$ symmetry, $c_j \rightarrow e^{i\alpha} c_j$, $\alpha \in \mathbb{R}$, associated with conservation of the total number of fermions N . Moreover, the model is integrable and the exact spectrum for arbitrary values of V can be calculated from the Bethe ansatz solution [57,58]. There is a gapless phase extending between $-2 < V \leq 2$. At $V = 2$ the model is equivalent to the $SU(2)$ -symmetric Heisenberg spin chain [57].

A useful starting point for analytical approximations is the noninteracting model with $V = 0$. In this case, the elementary excitations are free fermions with dispersion relation $\epsilon_0(k) = -2t \cos k - \mu$. Low-energy excitations are particles and holes with momentum close to the Fermi points, $k \approx \pm k_F$. The Fermi momentum is related to the average density by $k_F = \pi N / (La_0)$, where a_0 is the lattice spacing.

At weak coupling, $V/t \ll 1$, standard bosonization can be used to derive an effective low-energy theory for model (2), see, e.g., Refs. [25,26,59]. One starts by taking the continuum limit and projecting the fermionic field onto states with momentum near the Fermi points. This leads to the right- and left-moving components in the mode expansion:

$$c_j \rightarrow \sqrt{a_0} [e^{ik_F x} R(x) + e^{-ik_F x} L(x)]. \quad (3)$$

The effective Hamiltonian in terms of R and L fermions reads

$$\mathcal{H} = \int dx [-v' R^\dagger i \partial_x R + v' L^\dagger i \partial_x L + g R^\dagger R L^\dagger L + \mathcal{H}_{\text{irr}}(x)], \quad (4)$$

where all operators are normal ordered with respect to the noninteracting Dirac sea. To first order in V , we have the parameters $v' \approx 2ta_0 \sin(k_F a_0) [1 + \frac{V}{\pi t} \sin(k_F a_0)]$ and $g \approx 4Va_0 \sin^2(k_F a_0)$. The coupling constant g is the only marginal interaction. The term $\mathcal{H}_{\text{irr}}(x)$ contains nonlinear dispersion terms and other interactions which are irrelevant in the renormalization group (RG) sense. In the standard Luttinger liquid approach, this term is dropped, which corresponds to linearizing the dispersion around the Fermi points $\pm k_F$.

The bosonization formula for chiral spinless fermions reads

$$R(x) = \frac{\eta}{\sqrt{2\pi}} e^{-\frac{i}{\sqrt{2}} \varphi(x)}, \quad (5)$$

$$L(x) = \frac{\bar{\eta}}{\sqrt{2\pi}} e^{\frac{i}{\sqrt{2}} \bar{\varphi}(x)}, \quad (6)$$

where $\eta, \bar{\eta}$ are Majorana fermions and $\varphi(x), \bar{\varphi}(x)$ are chiral bosons that obey the commutation relations

$$[\varphi(x), \bar{\varphi}(y)] = 0, \quad (7)$$

$$[\varphi(x), \varphi(y)] = 2\pi i \text{sgn}(x - y) = -[\bar{\varphi}(x), \bar{\varphi}(y)]. \quad (8)$$

Throughout this paper we use “CFT normalizations” for bosonic vertex operators:

$$\langle e^{i\alpha\varphi(x)} e^{-i\alpha\varphi(y)} \rangle = \frac{1}{(x - y)^{2\alpha^2}}. \quad (9)$$

A consequence of employing these conventions is that vertex operators are dimensionful:

$$\dim(e^{i\alpha\varphi(x)}) = \text{length}^{-\alpha^2}. \quad (10)$$

We also define the canonical bosonic field $\Phi(x)$ and its dual $\Theta(x)$ by

$$\Phi(x) = \varphi(x) + \bar{\varphi}(x), \quad (11)$$

$$\Theta(x) = \varphi(x) - \bar{\varphi}(x), \quad (12)$$

which obey

$$[\Phi(x), \Theta(x')] = 4\pi i \text{sgn}(x - x'). \quad (13)$$

Bosonization of Eq. (4) then leads to the Hamiltonian

$$\mathcal{H} = \int dx [\mathcal{H}_{\text{LL}}(x) + \mathcal{H}_{\text{irr}}(x)]. \quad (14)$$

The first term,

$$\mathcal{H}_{\text{LL}}(x) = \frac{v}{16\pi} \left[K(\partial_x \Theta)^2 + \frac{1}{K}(\partial_x \Phi)^2 \right], \quad (15)$$

is the Luttinger model. The velocity v and the Luttinger parameter K are given to first order in V by $v \approx v'$ and $K \approx 1 - \frac{V}{\pi t} \sin k_F$. The bosonic fields describe the collective low-energy density mode of the quantum fluid. The uniform part of the density operator is related to $\Phi(x)$ by the bosonization relation

$$Q(x) = R^\dagger(x)R(x) + L^\dagger(x)L(x) \sim -\frac{1}{\pi\sqrt{8}}\partial_x \Phi(x). \quad (16)$$

The total charge operator is given by the integral

$$q = \int_{-\infty}^{+\infty} dx Q(x). \quad (17)$$

Thus, an elementary excitation with charge $q = 1$ corresponds to a kink of amplitude $\pi\sqrt{8}$ in the bosonic field $\Phi(x)$. As is well known, the model in Eq. (15) correctly captures the long-distance asymptotic decay of correlation functions for any 1D system in the Luttinger liquid universality class [25–27].

The limitations of Luttinger liquid theory appear when one considers dynamical response functions at small but finite frequency and momentum. At finite energy scales, it becomes necessary to take the irrelevant perturbations \mathcal{H}_{irr} to the Luttinger model into account. At weak coupling and in the absence of particle-hole symmetry (i.e., away from half-filling in the lattice model), the leading corrections in Eq. (4) are the dimension-three operators

$$\begin{aligned} \mathcal{H}_{\text{irr}} = & -\frac{1}{2\tilde{m}} (R^\dagger \partial_x^2 R + L^\dagger \partial_x^2 L) \\ & + g_3 (R^\dagger R L^\dagger i \partial_x L - L^\dagger L R^\dagger i \partial_x R + \text{H.c.}). \end{aligned} \quad (18)$$

Here, we have introduced $\tilde{m}^{-1} \approx m^{-1} + \frac{V a_0^2}{\pi} \sin 2k_F$, with $m^{-1} = 2t a_0^2 \cos k_F$ the inverse free fermion mass, and $g_3 \approx V a_0^2 \sin 2k_F$. Bosonizing these irrelevant terms we obtain cubic boson-boson interactions

$$\begin{aligned} \mathcal{H}_{\text{irr}} = & \lambda_3^+ \partial_x \Phi [(\partial_x \Phi)^2 + (\partial_x \Theta)^2] \\ & + \lambda_3^- \partial_x \Phi [(\partial_x \Phi)^2 - (\partial_x \Theta)^2], \end{aligned} \quad (19)$$

with $\lambda_3^+ \approx -\frac{1}{48\sqrt{2\pi}}(\frac{1}{m} + \frac{g_3}{\pi})$ and $\lambda_3^- \approx \frac{1}{96\sqrt{2\pi}}(\frac{1}{m} - \frac{2g_3}{\pi})$. While the bosonic representation allows one to take the marginal interaction g into account exactly, perturbation theory in the nonlinear boson interactions (19) suffers from infrared

divergences [34,46]. The latter are associated with the huge degeneracy of states in the linear dispersion approximation: all states with an arbitrary number of bosons moving in the same direction carrying the same total momentum are degenerate [34,46].

A way to circumvent these difficulties in analyzing the nonlinear bosonic theory is suggested by reverting to the fermionic representation (18). At the free fermion point, the irrelevant interaction vanishes, $g_3 = 0$, and one is left with the quadratic dispersion term with effective mass m . Taking the nonlinear dispersion into account in the free fermion model removes the degeneracy of particle-hole pairs that carry the same total momentum. One can then approach the problem from free fermions with nonlinear dispersion and include interactions perturbatively [28]. This approach reveals that the most pronounced effect of the interactions is to give rise to power-law singularities at the edges of the excitation spectrum. While a complete analytical solution of model (4) taking into account both band curvature and interaction is highly nontrivial, the edge singularities can be described by an effective impurity model in analogy with the x-ray edge problem [28,60].

Consider, for instance, the single-fermion spectral function

$$A(\omega, k) = -\frac{1}{\pi} \text{Im} G_{\text{ret}}(\omega, k), \quad (20)$$

where

$$G_{\text{ret}}(\omega, k) = -i \int_0^\infty dt e^{i\omega t} \sum_l e^{-ikla_0} \langle \psi_0 | \{c_{j+l}(t), c_j^\dagger\} | \psi_0 \rangle \quad (21)$$

is the retarded Green's function, with $|\psi_0\rangle$ the exact ground state. We can separate the negative- and positive-frequency parts of the spectral function:

$$A(\omega, k) = A_<(\omega, k) + A_>(\omega, k). \quad (22)$$

The Lehmann representation reads

$$A_<(\omega, k) = 2\pi \sum_n |\langle \psi_n | c_k | \psi_0 \rangle|^2 \delta(\omega + E_n - E_0), \quad (23)$$

$$A_>(\omega, k) = 2\pi \sum_n |\langle \psi_n | c_k^\dagger | \psi_0 \rangle|^2 \delta(\omega - E_n + E_0), \quad (24)$$

where c_k annihilates a fermion with momentum k and $|\psi_n\rangle$ denotes an exact eigenstate of the Hamiltonian with energy E_n . Let us focus on the negative-frequency part for $k < k_F$. For free fermions, we have $A_<^{(0)}(\omega, k) = \delta(\omega - \epsilon_0(k))$, where $\epsilon_0(k) < 0$ is the energy of the particle annihilated below the Fermi surface. When weak interactions are turned on, the renormalized fermion dispersion $\epsilon(k)$ becomes a threshold of the support of $A_<(\omega, k)$, such that a power-law singularity develops for $\omega < \epsilon(k)$. To describe the edge singularity for fixed $k < k_F$, we go back to the mode expansion in Eq. (3) and generalize it to include three patches of momentum:

$$c_j \rightarrow \sqrt{a_0} [e^{ik_F x} r(x) + e^{-ik_F x} l(x) + e^{ikx} \chi^\dagger(x)], \quad (25)$$

Here the ‘‘impurity field’’ $\chi^\dagger(x)$ creates a hole in a state with momentum close to k , within a subband of width $\Lambda \ll k_F - k$. The low-energy Fermi fields $r(x)$ and $l(x)$ are also defined with a cutoff of order Λ . In the case $q = k_F - k \ll k_F$, the field $l(x)$ can be regarded as the projection of $L(x)$ into

a narrower subband, while $R(x)$ is split into two separate subbands corresponding to the low-energy mode $r(x)$ and the “high-energy” mode $\chi(x)$. Restricting the energy window to the vicinity of the threshold with a single impurity, we now have to calculate the propagator of $\chi(x)$:

$$G_{\text{ret},<}(\omega, k) \approx -i \int_0^\infty dt e^{i\omega t} \int_{-\infty}^\infty dx \langle \psi_0 | \chi(0,0) \chi^\dagger(t,x) | \psi_0 \rangle. \quad (26)$$

At weak coupling, i.e., as long as the four-fermion interaction strength V is small, we can substitute Eq. (25) into Eq. (2) and bosonize the low-energy fields to derive an effective Hamiltonian for the single hole coupled to low-energy collective modes. The result is the mobile impurity model [38]

$$\mathcal{H}_{\text{imp}} = \int dx \left\{ \frac{v}{16\pi} \left[K(\partial_x \Theta)^2 + \frac{1}{K}(\partial_x \Phi)^2 \right] + \chi^\dagger(\varepsilon - iu\partial_x)\chi + \chi^\dagger \chi [f(q)\partial_x \varphi + \bar{f}(q)\partial_x \bar{\varphi}] \right\}, \quad (27)$$

where $\varepsilon \equiv -\varepsilon(k) > 0$ is the energy of the “deep hole” excitation, $u = \frac{d\varepsilon}{dk}$ is the velocity obtained by linearizing the dispersion around the center of the impurity subband, and $f(q)$ and $\bar{f}(q)$ are momentum-dependent impurity-boson couplings of order V . The calculation of the Green’s function in Eq. (21) is made possible by performing a unitary transformation that decouples the impurity from the low-energy modes:

$$U = e^{-i \int_{-\infty}^\infty dx [\gamma\varphi(x) + \bar{\gamma}\bar{\varphi}(x)] \chi^\dagger(x)\chi(x)}. \quad (28)$$

The bosonic fields transform as

$$\begin{aligned} \varphi^\circ(x) &= U\varphi(x)U^\dagger = \varphi(x) - 2\pi\gamma C(x), \\ \bar{\varphi}^\circ(x) &= U\bar{\varphi}(x)U^\dagger = \bar{\varphi}(x) + 2\pi\bar{\gamma}C(x), \end{aligned} \quad (29)$$

where

$$C(x) = \int_{-\infty}^\infty dy \operatorname{sgn}(x-y) \chi^\dagger(y)\chi(y). \quad (30)$$

The transformed impurity field is

$$\begin{aligned} d(x) &= U\chi(x)U^\dagger \\ &= \chi(x) e^{i[\gamma\varphi(x) + \bar{\gamma}\bar{\varphi}(x)]} e^{-i\pi(\gamma^2 - \bar{\gamma}^2)C(x)}. \end{aligned} \quad (31)$$

Note that the impurity density is invariant under the unitary transformation, i.e., $\chi^\dagger(x)\chi(x) = d^\dagger(x)d(x)$.

We choose the parameters $\gamma, \bar{\gamma}$ as the solution of

$$\begin{pmatrix} f \\ \bar{f} \end{pmatrix} = \begin{pmatrix} -v_+ + u & -v_- \\ v_- & v_- - u \end{pmatrix} \begin{pmatrix} \gamma \\ \bar{\gamma} \end{pmatrix}, \quad (32)$$

where

$$v_\pm = \frac{v}{2} \left(K \pm \frac{1}{K} \right). \quad (33)$$

With this choice, the Hamiltonian becomes noninteracting:

$$\begin{aligned} H_{\text{imp}} &= \int dx \left\{ \frac{v}{16\pi} \left[K(\partial_x \Theta^\circ)^2 + \frac{1}{K}(\partial_x \Phi^\circ)^2 \right] \right. \\ &\quad \left. + d^\dagger(\varepsilon - iu\partial_x)d + \dots \right\}, \end{aligned} \quad (34)$$

where \dots stands for irrelevant operators, which are neglected in the impurity model (since they only introduce subleading corrections to edge singularities). On the other hand, the expression in Eq. (26) now becomes

$$\begin{aligned} G_{\text{ret},<}(\omega, k) &\approx -i \int_0^{+\infty} dt e^{i\omega t} \int_{-\infty}^\infty dx \langle d(0,0) d^\dagger(t,x) \rangle_0 \\ &\quad \times \langle F(0,0) F^\dagger(t,x) \rangle_0, \end{aligned} \quad (35)$$

where $\langle \rangle_0$ denotes the expectation value in the noninteracting ground state $|\psi_0\rangle = U|\psi_0\rangle$ and $F(x)$ is the string operator

$$F(x) = e^{i[\gamma\varphi^\circ(x) + \bar{\gamma}\bar{\varphi}^\circ(x)]}. \quad (36)$$

The correlation function in Eq. (35) can then be calculated by standard methods [54]. The important point is that the scaling dimension of the operator $F(x)$ changes continuously as a function of $\gamma, \bar{\gamma}$. As a result, the effective impurity model predicts a power-law singularity in the spectral function,

$$A_{<}(\omega, k) \sim \theta(\varepsilon(k) - \omega) |\varepsilon(k) - \omega|^{-1+2(\gamma^2 + \bar{\gamma}^2)}. \quad (37)$$

Importantly, the impurity mode $\chi(x)$ in Eq. (27) carries charge $q = 1$ because it is defined from the original fermion c_j at the noninteracting point. This is the particle that can be identified with an elementary excitation in the Bethe ansatz solution for the integrable model. From the exact S matrix it is known that interactions between these elementary excitations increase as V increases. Particularly at the $SU(2)$ point, $V = 2$, the elementary excitations are rather strongly interacting. By contrast, the transformed impurity operator $d(x) = \chi(x)F(x)$ carries a fractional charge that depends on the interaction strength, since the string $F(x)$ in general does not commute with the charge operator in Eq. (17).

In the low-energy limit, an alternative approach to obtain the edge singularity in the spectral function was put forward in Ref. [44]. In this approach, one starts by introducing fermionic quasiparticles that are asymptotically free at low energies. In our notation, the idea is to define chiral bosons $\phi, \bar{\phi}$ by

$$\Phi(x) = \sqrt{K}(\phi + \bar{\phi}), \quad (38)$$

$$\Theta(x) = \frac{1}{\sqrt{K}}(\phi - \bar{\phi}). \quad (39)$$

In terms of these, the Luttinger model (15) reads

$$\mathcal{H}_{\text{LL}}(x) = \frac{v}{8\pi} [(\partial_x \phi)^2 + (\partial_x \bar{\phi})^2]. \quad (40)$$

The quasiparticles $\tilde{R}(x)$ and $\tilde{L}(x)$ are defined by

$$\tilde{R}(x) = \frac{\eta}{\sqrt{2\pi}} e^{-\frac{i}{\sqrt{2}}\phi(x)}, \quad (41)$$

$$\tilde{L}(x) = \frac{\bar{\eta}}{\sqrt{2\pi}} e^{\frac{i}{\sqrt{2}}\bar{\phi}(x)}. \quad (42)$$

The commutator with the charge operator yields

$$[q, \tilde{R}^\dagger(x)] = \sqrt{K} \tilde{R}^\dagger(x), \quad [q, \tilde{L}^\dagger(x)] = \sqrt{K} \tilde{L}^\dagger(x). \quad (43)$$

Thus the quasiparticles carry charge \sqrt{K} . On the other hand, this refermionization procedure removes the marginal interaction between the quasiparticles since the chiral modes are decoupled in Eq. (40) [29,44]. The leading interaction is then represented by the irrelevant operator g_3 in Eq. (18), which

can be neglected as a first approximation in the low-energy limit. The relation between the original right-moving fermion and the new quasiparticle is

$$\tilde{R}(x) = R(x)F_0(x), \quad (44)$$

where $F_0(x)$ is the limit $q = k_F - k \rightarrow 0$ of the string operator in Eq. (36). At this point a noninteracting impurity mode $\tilde{\chi}(x)$ can be introduced by projecting the free field $\tilde{R}(x)$ into low-energy and high-energy subbands. This leads to a universal result for the exponent in the vicinity of the threshold, $|\omega - \epsilon(k)| \ll q^2/\tilde{m}$, which corresponds to Eq. (37) with parameters $\gamma = \frac{1}{\sqrt{2}}(1 - \frac{1}{2\sqrt{K}} - \frac{\sqrt{K}}{2})$ and $\tilde{\gamma} = \frac{1}{\sqrt{2}}(\frac{1}{2\sqrt{K}} - \frac{\sqrt{K}}{2})$. This result differs from the prediction of the linear theory [44].

In summary, there are two possible paths towards calculating edge exponents in the nLL theory for spinless fermions: (i) starting with free fermions, one defines low-energy and impurity subbands, and then turns on interactions between the elementary excitations in the impurity model; after that, the interaction with the impurity is removed by a unitary transformation, which introduces the string operator in the correlation function; or (ii) starting from the Luttinger model for interacting fermions, one refermionizes into weakly interacting quasiparticles, which differ from the original fermions by a string operator, and then projects the quasiparticles into low-energy and impurity subbands. The projection onto the impurity model is well controlled in both paths because the model of interacting spinless fermions is smoothly connected with the free model, i.e., the parameters $\gamma, \tilde{\gamma}$, which quantify the scattering between high-energy and low-energy particles, vanish continuously as $V \rightarrow 0$. However, it is important to emphasize the difference between the original fermions, which carry unit charge of the U(1) symmetry, and the quasiparticles with fractional charge. While the latter are always weakly interacting in the low-energy limit, the fermions that carry the correct quantum numbers become strongly interacting even at low energies as V increases.

Once the low-energy, weak-coupling regime is well understood, the impurity model of nLL theory can be extended phenomenologically to high energies, strong interactions and thresholds with more than one impurity, as has indeed been done successfully for spinless fermions [54].

III. SPINFUL FERMIONS

As we have seen above, the spinless case is most easily understood by considering the vicinity of noninteracting fermions. The situation is very different in the spinful case. In order to understand this point in some detail, let us consider the particular example of the 1D Hubbard model

$$H_{\text{Hub}} = -t \sum_{j=1}^L \sum_{\sigma} (c_{j,\sigma}^{\dagger} c_{j+1,\sigma} + \text{H.c.}) + U \sum_j n_{j,\uparrow} n_{j,\downarrow}, \quad (45)$$

where $c_{j,\sigma}$ annihilates a fermion with spin $\sigma = \uparrow, \downarrow$ at site j , $n_{j,\sigma} = c_{j,\sigma}^{\dagger} c_{j,\sigma}$ is the number operator, and $U \geq 0$ is the strength of the on-site repulsion. We work at fixed density below half-filling with zero magnetization, $N_{\uparrow} = N_{\downarrow} < L/2$. In this case, the model has a global $U(1) \otimes SU(2)$ symmetry. Let us focus first on the limit of weak interactions $U/t \ll 1$ and low

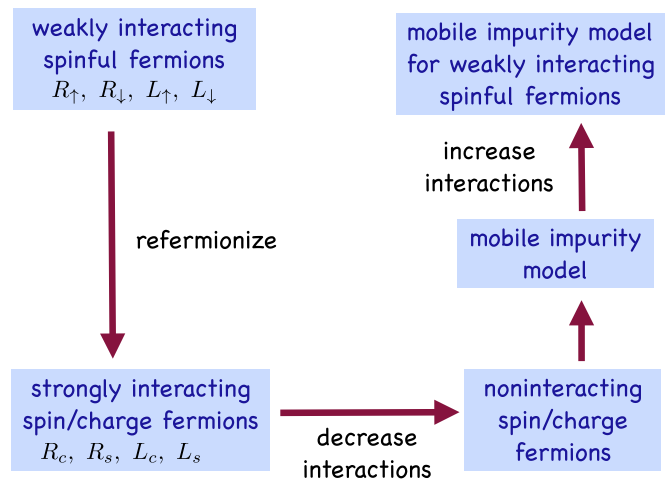


FIG. 1. (Color online) Strategy map for calculating edge exponents in nonlinear Luttinger liquid theory for spinful fermions in the low-energy limit. See the main text for details.

energies. It is well known [7] that the low-energy degrees of freedom are collective spin and charge modes respectively, i.e.,

$$H_{\text{Hub}} \longrightarrow \mathcal{H}_{\text{charge}} + \mathcal{H}_{\text{spin}} + \dots, \quad (46)$$

where the dots denote additional terms that are irrelevant in the renormalization group sense. Crucially, as H_{Hub} is spin rotationally symmetric, $\mathcal{H}_{\text{spin}}$ must exhibit a spin SU(2) symmetry. In order to parallel our analysis in the spinless case, we wish to express $\mathcal{H}_{\text{spin}}$ in terms of fermionic fields carrying spin quantum numbers $\pm 1/2$. This is possible in an SU(2)-symmetric way only if the fermions are *strongly interacting*, i.e., the situation is similar to the $V = 2$ case for spinless fermions. In the charge sector the situation is analogous unless we work at very low electron densities. In order to generalize the mobile impurity model construction reviewed in Sec. II to the spinful case, we therefore cannot work with weakly interacting spinful fermions, but require a model that gives rise to noninteracting fermions describing the collective spin and charge degrees of freedom. As such a model is not known, we proceed along the lines sketched in Fig. 1.

1. Starting with weakly interacting spinful fermions at low energies, we derive the corresponding model of strongly interacting spin and charge fermions.

2. We then decrease the interactions in the spin and charge fermion model, and derive a low-energy effective Hamiltonian in the vicinity of the “Luther-Emery point” [61] where the spin/charge fermions become noninteracting.

3. Having completed this construction, we are in a position to construct mobile impurity models by following the logic employed in the spinless case.

4. Having constructed a suitable mobile impurity model, we may calculate threshold exponents by standard methods.

5. Through an appropriate tuning of the parameters defining our mobile impurity model, we may analyze the case of weakly interacting SU(2)-invariant spinful fermions. This is analogous to the analysis of strongly interacting spinless fermions with SU(2) symmetry based on a mobile impurity model formulated at weak coupling.

A key ingredient in our approach is our ‘‘Luther-Emery model’’ of noninteracting holons and spinons. An obvious question is what such a theory might look like in terms of interacting spinful fermions. We address this issue in Sec. VII.

A. Bosonization at weak coupling

As our point of departure we choose a general extended Hubbard model below half-filling, where we allow fairly general electron-electron interactions in addition to (45), provided that they are invariant under the following symmetries:

$$\begin{aligned} & \text{U(1)} \otimes \text{U(1)} \text{ transformations in the charge and spin sectors} \\ & c_{j,\sigma} \rightarrow e^{i\alpha_\sigma} c_{j,\sigma}, \alpha_\sigma \in \mathbb{R}; \\ & \text{spin reflection } c_{j,\uparrow} \leftrightarrow c_{j,\downarrow}; \\ & \text{site parity } c_{j,\sigma} \rightarrow c_{-j,\sigma}; \\ & \text{translations } c_{j,\sigma} \rightarrow c_{j+1,\sigma}. \end{aligned}$$

The kind of lattice model we have in mind is of the form

$$\begin{aligned} H = & H_{\text{Hub}} + \sum_{r \geq 1} \sum_j V_r n_j n_{j+r} \\ & + \sum_{r \geq 1} \sum_j (J_r \mathbf{S}_j \cdot \mathbf{S}_{j+r} + J_r^z S_j^z S_{j+r}^z), \end{aligned} \quad (47)$$

where the coupling constants $\{V_r, J_r, J_r^z\}$ must be such that the model remains in a spin-charge-separated quantum critical phase. Lattice models of this type can be bosonized by standard methods [26,27]. The generalization of Haldane’s bosonization formulas [62] to the spinful case is

$$\begin{aligned} c_{j,\sigma} \sim & \sqrt{a_0} \sum_{n,m \in \mathbb{Z}} \Gamma_{n,m}^{(\sigma)} A_{n,m} e^{ik_F x(1-4n-2m)} \\ & \times e^{-\frac{i}{2}\varphi_c(x) - \frac{i}{2}s_\sigma \varphi_s(x)} e^{i\frac{2n+m}{2}\Phi_c(x)} e^{-is_\sigma \frac{m}{2}\Phi_s(x)}. \end{aligned} \quad (48)$$

Here, $s_\uparrow = 1 = -s_\downarrow$, a_0 is a short-distance cutoff, $x = ja_0$, $k_F = \pi N_\uparrow / (La_0)$ is the Fermi momentum, $A_{n,m}$ are nonuniversal amplitudes and $\Gamma_{n,m}^{(\sigma)} \equiv \eta_\sigma (\eta_\sigma \bar{\eta}_\sigma \eta_{\bar{\sigma}} \bar{\eta}_{\bar{\sigma}})^n (\eta_{\bar{\sigma}} \bar{\eta}_{\bar{\sigma}})^m$ are Klein factors (and we use notations where, e.g., $\uparrow = \downarrow$) that ensure the correct anticommutation relations. The bosonic fields

$$\Phi_\alpha(x) = \varphi_\alpha(x) + \bar{\varphi}_\alpha(x), \quad (49)$$

$$\Theta_\alpha(x) = \varphi_\alpha(x) - \bar{\varphi}_\alpha(x), \quad (50)$$

with $\alpha = c, s$, obey the commutation relations

$$[\Phi_\alpha(x), \Theta_{\alpha'}(x')] = 4\pi i \delta_{\alpha,\alpha'} \text{sgn}(x - x'). \quad (51)$$

We note that in the CFT normalizations (9) the amplitudes $A_{n,m}$ are dimensionful, i.e., they are proportional to appropriate powers of the lattice spacing a_0 .

In the spin-charge separated Luttinger liquid phase, the low-energy effective Hamiltonian for extended Hubbard models of the type (47) is

$$\mathcal{H} = \int dx [\mathcal{H}_{\text{LL}}(x) + \mathcal{H}_{\text{irr}}(x)], \quad (52)$$

$$\mathcal{H}_{\text{LL}}(x) = \sum_{\alpha=c,s} \frac{v_\alpha}{16\pi} \left[K_\alpha (\partial_x \Theta_\alpha)^2 + \frac{1}{K_\alpha} (\partial_x \Phi_\alpha)^2 \right], \quad (53)$$

$$\begin{aligned} \mathcal{H}_{\text{irr}}(x) = & \lambda_1 \cos \Phi_s + \lambda_2 \partial_x \Phi_c \cos \Phi_s \\ & + \sum_{\alpha=c,s} \lambda_{3,\alpha}^\pm \partial_x \Phi_c [(\partial_x \Phi_\alpha)^2 \pm (\partial_x \Theta_\alpha)^2] \\ & + \lambda_4 \partial_x \Phi_s \partial_x \Theta_s \partial_x \Theta_c + \dots \end{aligned} \quad (54)$$

Here, v_α are the velocities of the collective charge and spin modes and K_α the corresponding Luttinger parameters. The contributions \mathcal{H}_{irr} are irrelevant in the renormalization group sense. A complete list of irrelevant operators with scaling dimensions of at most four (for $K_s = 1$) is given in Appendix A. The velocities v_α and Luttinger parameters K_α can be calculated exactly for the Hubbard model, but Eq. (52) is generic for spinful Luttinger liquids if we regard v_α and K_α as phenomenological parameters. We note that, as a consequence of spin reflection symmetry, marginal interactions coupling spin and charge such as

$$\partial_x \Phi_s(x) \partial_x \Phi_c(x) \quad (55)$$

are not allowed. Hence the collective degrees of freedom at low energies are described in terms of pure spin and pure charge modes, rather than linear combinations thereof (which would be the case in presence of a magnetic field, see, e.g., Ref. [63]).

B. Refermionizing in terms of spin and charge fields

The next step is to refermionize (52) in terms of spin and charge fermion fields. In order to see how this should be done, we consider the limit of vanishing interactions. Here the bosonization formulas simplify to ($\sigma = \uparrow, \downarrow$)

$$\begin{aligned} c_{j,\sigma} & \rightarrow \sqrt{a_0} [e^{ik_F x} R_\sigma(x) + e^{-ik_F x} L_\sigma(x)], \\ R_\sigma(x) & \sim \frac{\eta_\sigma}{\sqrt{2\pi}} e^{-\frac{i}{2}\varphi_c(x) - \frac{i}{2}s_\sigma \varphi_s(x)}, \\ L_\sigma(x) & \sim \frac{\bar{\eta}_\sigma}{\sqrt{2\pi}} e^{\frac{i}{2}\bar{\varphi}_c(x) + \frac{i}{2}s_\sigma \bar{\varphi}_s(x)}, \end{aligned} \quad (56)$$

where $s_\uparrow = -s_\downarrow = 1$. The idea is to decompose the right-moving spin-up electron into a right-moving holon field R_c and a right-moving spinon field R_s in the form

$$R_\uparrow(x) \sim R_c(x) e^{i(\text{charge string})} R_s(x) e^{i(\text{spin string})}. \quad (57)$$

In a pure Luttinger liquid, there are infinitely many acceptable choices for R_α and string operators in Eq. (57). In Refs. [51,52], the fermions R_α are chosen so as to have scaling dimension 1/2, in analogy with the procedure in the spinless case, see Eqs. (41) and (42). This choice is such that the particles are asymptotically free at low energies. However, they then carry fractional spin and charge quantum numbers. Such a choice is not the most natural one for our purposes: it is known that the scaling limit of the Hubbard model is given by the U(1) Thirring model [SU(2) at half-filling], see, e.g., Ref. [26]. The U(1) Thirring model is integrable, and the elementary excitations are known to be strongly interacting fermionic spinless holons and neutral spinons (with a known S matrix) carrying charge $\mp e$ and spin $\pm 1/2$, respectively. The principle guiding our construction is that charge and spin fermions created by R_c^\dagger and R_s^\dagger should carry the same quantum numbers as the elementary holon and spin excitations. The

U(1) charges corresponding to these quantum numbers are

$$q_\alpha = \int_{-\infty}^{+\infty} dx Q_\alpha(x), \quad (58)$$

where

$$\begin{aligned} Q_c(x) &= \sum_{\sigma=\uparrow,\downarrow} [R_\sigma^\dagger(x)R_\sigma(x) + L_\sigma^\dagger(x)L_\sigma(x)], \\ Q_s(x) &= \sum_{\sigma=\uparrow,\downarrow} s_\sigma [R_\sigma^\dagger(x)R_\sigma(x) + L_\sigma^\dagger(x)L_\sigma(x)]. \end{aligned} \quad (59)$$

As usual, these expressions are to be understood in terms of a standard point splitting and normal ordering prescription. We now require

$$\begin{aligned} Q_c(x) &= R_c^\dagger(x)R_c(x) + L_c^\dagger(x)L_c(x), \\ Q_s(x) &= R_s^\dagger(x)R_s(x) + L_s^\dagger(x)L_s(x), \end{aligned} \quad (60)$$

which ensure that the spin and charge fermions have the desired U(1) charges:

$$[q_\alpha, R_\alpha^\dagger(x)] = R_\alpha^\dagger(x), \quad [q_\alpha, L_\alpha^\dagger(x)] = L_\alpha^\dagger(x). \quad (61)$$

Our refermionization prescription then reads

$$\begin{aligned} R_\uparrow(x) &\sim \eta_\uparrow \mathcal{O}_c(x) \mathcal{O}_s(x), \\ R_\downarrow(x) &\sim \eta_\downarrow \mathcal{O}_c(x) \mathcal{O}_s^\dagger(x), \\ \mathcal{O}_\alpha(x) &\sim R_\alpha(x) e^{-\frac{i\pi}{2} \int_{-\infty}^x dx' Q_\alpha(x')}. \end{aligned} \quad (62)$$

Analogous relations hold for left-moving fermions. One issue that arises here is that $n_s(x) = \int_{-\infty}^x dx' Q_s(x')$ is the number of spinons on the interval $[-\infty, x]$, and therefore string operators of the form $\exp[i\alpha n_s(x)]$ should be 2π -periodic functions of α . When bosonizing string operators naively this periodicity is lost. A simple way of dealing with this issue is via the replacement [64]

$$\exp[i\alpha n_s(x)] \longrightarrow \sum_m \exp[i(2\pi m + \alpha)n_s(x)]. \quad (63)$$

The operators $\mathcal{O}_\alpha(x)$ fulfill braiding relations for $x \neq y$:

$$\mathcal{O}_\alpha(x)\mathcal{O}_\alpha(y) = e^{-\frac{i\pi}{2} \text{sgn}(x-y)} \mathcal{O}_\alpha(y)\mathcal{O}_\alpha(x). \quad (64)$$

The low-energy effective Hamiltonian (52) is expressed in terms of our fermionic charge and spin fields as

$$\begin{aligned} \mathcal{H} &= \int dx [\mathcal{H}_c(x) + \mathcal{H}_s(x) + \mathcal{H}_{cs}(x)], \\ \mathcal{H}_c &= R_c^\dagger(-iv'_c\partial_x - \eta\partial_x^2)R_c + L_c^\dagger(iv'_c\partial_x - \eta\partial_x^2)L_c \\ &\quad + g_{c,0}R_c^\dagger R_c L_c^\dagger L_c + \dots, \\ \mathcal{H}_s &= R_s^\dagger(-iv'_s\partial_x + i\zeta\partial_x^3)R_s + L_s^\dagger(iv'_s\partial_x - i\zeta\partial_x^3)L_s \\ &\quad + g_{s,0}R_s^\dagger R_s L_s^\dagger L_s + g_{s,1}(R_s^\dagger L_s + L_s^\dagger R_s) + \dots, \\ \mathcal{H}_{cs} &= g_1(R_c^\dagger R_c + L_c^\dagger L_c)(R_s^\dagger L_s + \text{H.c.}) + \dots \end{aligned} \quad (65)$$

A crucial feature of this expression is that the coupling constants of the marginal interactions,

$$g_{\alpha,0} \sim 2\pi v_\alpha \left(\frac{1}{4K_\alpha} - K_\alpha \right), \quad (66)$$

are $\mathcal{O}(1)$ at weak coupling $K_\alpha \rightarrow 1$. Moreover, $g_{s,0}$ is always large as long as the spin SU(2) symmetry is unbroken, as in this case the Luttinger parameter is fixed at $K_s = 1$. This implies that the spin and charge fermions are *strongly interacting*. This is consistent with known results for the exact S matrix of the Hubbard model [8–10]. Moreover, the spin sector of (65) describes a massive Thirring model perturbed by irrelevant operators, which is precisely what one would expect on the basis of the known S matrices for the Hubbard model [65].

C. Bosonic representation of charge and spin fermions

Our spin and charge fermion fields can be bosonized by standard methods. Introducing chiral charge and spin ($\alpha = c, s$) Bose fields φ_α^* , $\bar{\varphi}_\alpha^*$, and ignoring higher harmonics, we have

$$R_\alpha(x) \sim \frac{\eta_\alpha}{\sqrt{2\pi}} e^{-\frac{i}{\sqrt{2}}\varphi_\alpha^*(x)}, \quad L_\alpha(x) \sim \frac{\bar{\eta}_\alpha}{\sqrt{2\pi}} e^{\frac{i}{\sqrt{2}}\bar{\varphi}_\alpha^*(x)}, \quad (67)$$

where $\eta_\alpha, \bar{\eta}_\alpha$ are Klein factors fulfilling anticommutation relations $\{\eta_\alpha, \eta_\beta\} = 2\delta_{\alpha,\beta} = \{\bar{\eta}_\alpha, \bar{\eta}_\beta\}$, $\{\eta_\alpha, \eta_\beta\} = 0$. Bosonizing the spin and charge fermions leads to the following expressions for the original right- and left-moving spinful fermions:

$$\begin{aligned} R_\uparrow(x) &\propto \prod_{\alpha=c,s} e^{-\frac{i}{\sqrt{2}}\varphi_\alpha^*(x) + \frac{i}{4\sqrt{2}}\Phi_\alpha^*(x)}, \\ L_\uparrow(x) &\propto \prod_{\alpha=c,s} e^{\frac{i}{\sqrt{2}}\bar{\varphi}_\alpha^*(x) - \frac{i}{4\sqrt{2}}\Phi_\alpha^*(x)}. \end{aligned} \quad (68)$$

The new Bose fields $\varphi_\alpha^*, \bar{\varphi}_\alpha^*$ are related to the usual spin and charge bosons (52) by a canonical transformation

$$\Phi_\alpha = \frac{\Phi_\alpha^*}{\sqrt{2}}, \quad \Theta_\alpha = \sqrt{2}\Theta_\alpha^*. \quad (69)$$

Given (69), it is straightforward to rewrite (52) in terms of the new Bose fields

$$\begin{aligned} \mathcal{H} &= \int dx \left\{ \sum_\alpha \frac{v'_\alpha}{16\pi} [(\partial_x \Theta_\alpha^*)^2 + (\partial_x \Phi_\alpha^*)^2] \right. \\ &\quad + \sum_\alpha \lambda_\alpha [(\partial_x \Theta_\alpha^*)^2 - (\partial_x \Phi_\alpha^*)^2] + \lambda_1 \cos(\Phi_s^*/\sqrt{2}) \\ &\quad \left. + \frac{\lambda_2}{\sqrt{2}} \partial_x \Phi_c^* \cos(\Phi_s^*/\sqrt{2}) + \dots \right\}, \end{aligned} \quad (70)$$

where $v'_\alpha = v_\alpha(K_\alpha + \frac{1}{4K_\alpha})$ and $\lambda_\alpha = \frac{v_\alpha}{16\pi}(K_\alpha - \frac{1}{4K_\alpha})$.

IV. LUTHER-EMERY (LE) POINT FOR SPIN AND CHARGE

A particular case of the family of Hamiltonians (65) describes a free theory of *noninteracting* gapless fermionic spinons and holons. This LE point for both spin and charge corresponds to

$$\begin{aligned} \mathcal{H}_{\text{LE}} &= \int dx [R_c^\dagger(-iv'_c\partial_x - \eta\partial_x^2 + \dots)R_c \\ &\quad + L_c^\dagger(iv'_c\partial_x - \eta\partial_x^2 + \dots)L_c \end{aligned}$$

$$\begin{aligned}
 &+ R_s^\dagger (-i v_s' \partial_x + i \zeta \partial_x^3 + \dots) R_s \\
 &+ L_s^\dagger (i v_s' \partial_x - i \zeta \partial_x^3 + \dots) L_s]. \quad (71)
 \end{aligned}$$

Here we have included the quadratic (cubic) term in the holon (spinon) dispersion to emphasize the nonlinearity. In order to realize a Hamiltonian of this form fine-tuning a number of couplings is required, as can be seen by analyzing the stability of (71) to perturbations.

A. Stability of the LE point

An obvious question is to what extent the LE point is stable. The most important perturbations to (71) are

$$\begin{aligned}
 \mathcal{H}_{\text{pert}} = &\int dx [g_{c,0} R_c^\dagger R_c L_c^\dagger L_c \\
 &+ g_{s,1} (R_s^\dagger L_s + L_s^\dagger R_s) + g_{s,0} R_s^\dagger R_s L_s^\dagger L_s \\
 &+ g_1 (R_c^\dagger R_c + L_c^\dagger L_c) (R_s^\dagger L_s + \text{H.c.})]. \quad (72)
 \end{aligned}$$

In addition to (72) there are other, less relevant perturbations. A list of the ones with scaling dimension below four is given in Appendix B. The $g_{s,1}$ term in Eq. (72) is recognized as a mass term for spinons, and is the only strongly relevant perturbation. This implies that spinons are generically gapped, and in order to reach a LE point with gapless spinons *fine tuning* $g_{s,1} = 0$ is necessary. Assuming that this is possible, we are left with three perturbing operators of scaling dimension 2. While the $g_{s,0}$ and $g_{c,0}$ terms are scalar, the g_1 term carries nonzero Lorentz spin. In order to assess the stability of the LE point to these perturbations, we have carried out a renormalization group analysis. In principle, we need to work with different cut-offs for the charge and spin degrees of freedom. However, at one-loop logarithmic divergences are encountered only in the spin sector. We obtain RG equations of the form

$$\frac{dg_1}{d\ell} = \frac{1}{4\pi v_s} g_1 g_{s,0}, \quad \frac{dv_c}{d\ell} = -\frac{1}{2\pi^2 v_s} g_1^2, \quad (73)$$

$$\frac{dg_{c,0}}{d\ell} = -\frac{1}{\pi v_s} g_1^2, \quad \frac{dg_{s,0}}{d\ell} = \frac{dv_s}{d\ell} = 0, \quad (74)$$

where $\ell = \ln(L/a_0)$ and a_0 and L are short- and long-distance cutoffs, respectively. The RG equations are easily integrated,

$$\begin{aligned}
 g_{s,0}(\ell) &= g_{s,0}(\ell_0), \quad g_1(\ell) = g_1(\ell_0) e^{\frac{g_{s,0}(\ell_0)}{4\pi v_s(\ell_0)}(\ell-\ell_0)}, \\
 g_{c,0}(\ell) &= g_{c,0}(\ell_0) - \frac{2g_1^2(\ell_0)}{g_{s,0}(\ell_0)} \left[e^{\frac{g_{s,0}(\ell_0)}{2\pi v_s(\ell_0)}(\ell-\ell_0)} - 1 \right], \quad (75)
 \end{aligned}$$

and imply the following. (1) The spinon mass term is not produced under the RG flow if the bare coupling is initially set to zero. We have checked that this remains true at two loops. However, we cannot rule out that $g_{s,1}$ may be generated at higher orders and it is possible that setting it to zero requires fine tuning an infinite number of parameters in a lattice model. (2) The coupling $g_{s,0}$ does not flow under the RG. This remains true at two-loop order. Hence, to this order, $g_{s,0}$ needs to be fine-tuned to zero in order to reach the LE point. (3) If the initial value $g_{s,0}(\ell_0) < 0$, the coupling $g_1(\ell)$ flows to zero under the RG, while $g_{c,0}(\ell)$ flows to a constant value.

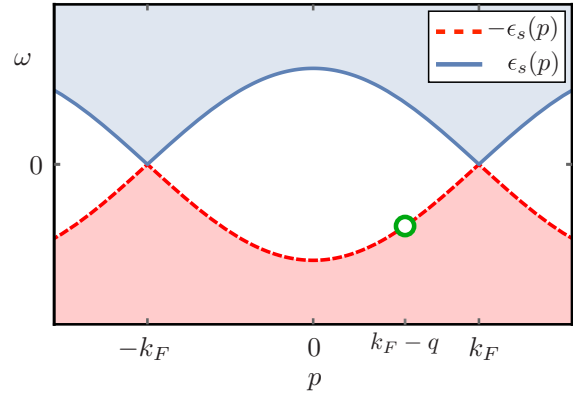


FIG. 2. (Color online) Support in the energy/momentum plane of excitations with the quantum numbers of an electron or hole. For commensurate band fillings, there is an absolute threshold that we take to follow the spinon/anti-spinon dispersions. Above the threshold, the single-particle spectral function is singular, and we aim to determine the threshold exponent of the negative-frequency part at a momentum $k_F - q$ (green circle).

B. Threshold singularities in the single electron spectral function

Given the low-energy Hamiltonian at the LE point (71), we are now in a position to derive a mobile impurity model, valid a priori at low energies. The usual continuity arguments suggest that the restriction to low energies can be relaxed and the model applied to energies of the order of the lattice scale t . Let us focus on the mobile impurity model relevant for analyzing the threshold behavior in the single-electron spectral function,

$$\begin{aligned}
 A(\omega, k) &= -\frac{1}{\pi} \text{Im} G_{\text{ret}}(\omega, k), \\
 G_{\text{ret}}(\omega, k) &= -i \int_0^\infty dt e^{i\omega t} \sum_l e^{-ikla_0} \\
 &\quad \times \langle \psi_0 | \{c_{j+l, \sigma}(t), c_{j, \sigma}^\dagger\} | \psi_0 \rangle, \quad (76)
 \end{aligned}$$

where $|\psi_0\rangle$ is the ground state.

For commensurate band fillings the spectral function has a threshold at low energies. To be specific, we will consider the case $v_s' < v_c'$, in which case the threshold corresponds to exciting a single high-energy spinon, while (anti)holon excitations have vanishing energy. The corresponding kinematics is sketched in Fig. 2. The negative frequency part of the spectral function at fixed momentum transfer $k = k_F - q$ exhibits a threshold singularity

$$A(\omega, k) = \begin{cases} 0 & \text{if } 0 > \omega > -\epsilon_s(k), \\ A_0 |\omega + \epsilon_s(k)|^\mu & \text{if } \omega \rightarrow -\epsilon_s(k). \end{cases} \quad (77)$$

Here, $\epsilon_s(k)$ denotes the spinon dispersion.

C. Threshold exponent at the LE point

Let us focus on momentum transfers $k_F - q$, where we take $0 < q \ll k_F$. Using the decomposition

$$c_\sigma \sim \sqrt{a_0} [e^{ik_F x} R_\sigma(x) + e^{-ik_F x} L_\sigma(x)], \quad (78)$$

we see that the relevant field theory correlator is

$$\begin{aligned} A(\omega, k_F - q) &\sim -i \int_0^\infty dt \int_{-\infty}^\infty dx e^{i\omega t + iqx} \\ &\quad \times \langle \psi_0 | \{ R_\uparrow(t, x), R_\uparrow^\dagger(0, 0) \} | \psi_0 \rangle \\ &= A_<(\omega, k_F - q) + A_>(\omega, k_F - q). \end{aligned} \quad (79)$$

Here, $A_>$ and $A_<$ are, respectively, the positive and negative frequency parts of the spectral function. Using (62), we arrive at the following expression for the latter:

$$\begin{aligned} A_<(\omega, k_F - q) &\sim -i \int_0^\infty dt \int_{-\infty}^\infty dx e^{i\omega t + iqx} \\ &\quad \times \prod_{\alpha=c,s} \langle \psi_0 | \mathcal{O}_\alpha^\dagger(0, 0) \mathcal{O}_\alpha(t, x) | \psi_0 \rangle. \end{aligned} \quad (80)$$

At the LE point, we are dealing with a free fermion theory. Hence correlation functions of the kind required in Eq. (80) can be expressed as Fredholm determinants [66], but we do not follow this route here. Instead, we construct a mobile impurity model and use it to extract the threshold exponent.

At the LE point spin and charge degrees are perfectly separated. As a consequence it is possible to construct a basis of energy eigenstates in the form

$$|n_c\rangle \otimes |n_s\rangle, \quad (81)$$

where $n_{c,s}$ are appropriate charge and spin quantum numbers. The correlators required in Eq. (80) then have Lehmann representations of the form

$$\sum_{n_\alpha} e^{iE_{n_\alpha} t - iP_{n_\alpha} x} |\langle n_\alpha | \mathcal{O}_\alpha(0, 0) | \psi_0 \rangle|^2, \quad \alpha = c, s. \quad (82)$$

The threshold singularity arises from excitations involving a single high-energy spinon with momentum q plus low-energy excitations in the charge and spin sectors. This means that the charge part of (80) can be calculated using bosonization. The bosonization identities (68) imply that

$$\mathcal{O}_c(x) \propto e^{-\frac{i}{\sqrt{2}} \varphi_c^*(x)} e^{\frac{i}{4\sqrt{2}} \Phi_c^*(x)}. \quad (83)$$

At the LE point the coupling constants λ_α , λ_1 , λ_2 in Eq. (70) vanish, and a simple calculation gives

$$\langle \mathcal{O}_c^\dagger(0, 0) \mathcal{O}_c(t, x) \rangle \propto (v'_c t - x)^{-\frac{1}{2}} (x^2 - v'_c{}^2 t^2)^{-\frac{1}{16}}. \quad (84)$$

In order to work out the contribution from the spin part, we follow Ref. [67]. We decompose the spin fermions into low-energy and mobile impurity parts:

$$\begin{aligned} R_s(x) &\sim r_s(x) + e^{-iqx} \chi_s^\dagger(x), \\ L_s(x) &\sim l_s(x), \end{aligned} \quad (85)$$

where χ_s^\dagger creates a hole in the spinon band. In terms of momentum modes,

$$R_s(x) \sim \int \frac{dp}{2\pi} e^{ipx} R_s(p), \quad (86)$$

this projection corresponds to

$$\begin{aligned} r_s(x) &\sim \int_{-\Lambda'}^{\Lambda'} \frac{dp}{2\pi} e^{ipx} R_s(p), \\ \chi_s^\dagger(x) &\sim \int_{q-\Lambda''}^{q+\Lambda''} \frac{dp}{2\pi} e^{i(p-q)x} R_s(p), \quad \Lambda'' \ll |q|. \end{aligned} \quad (87)$$

Substituting the decomposition (85) into our expression of the Hamiltonian density (71) and dropping oscillatory contributions under the integral, we arrive at the following mobile impurity model:

$$\begin{aligned} \mathcal{H}_{\text{MIM}}^{(0)} &= \int dx \sum_{\alpha=c,s} -i v'_\alpha (r_\alpha^\dagger \partial_x r_\alpha - l_\alpha^\dagger \partial_x l_\alpha) \\ &\quad + \int dx \chi_s^\dagger (\varepsilon_s - i u_s \partial_x + \dots) \chi_s. \end{aligned} \quad (88)$$

Here, we have introduced notations $\varepsilon_s = \varepsilon_s(k_F - q) \approx v'_s q + \zeta q^3 + \dots$ and $u_s = -\frac{d\varepsilon_s}{dk}|_{k_F-q} \approx v'_s + 3\zeta q^2$.

Next, we need to work out the projection of the operator \mathcal{O}_s on low-energy (r_s) and impurity (χ_s) degrees of freedom. Using that $r_s(x)$, $l_s(x)$, and $\chi_s(x)$ are slowly varying fields, we can approximate the string operator as

$$\begin{aligned} \mathcal{O}_s(x) &\sim [r_s(x) + e^{-iqx} \chi_s^\dagger(x)] e^{\frac{\pi}{2} [\frac{\varepsilon - iqx}{q} r_s^\dagger(x) \chi_s^\dagger(x) - \text{H.c.}]} \\ &\quad \times e^{-\frac{i\pi}{2} \int_{-\infty}^x dx' [r_s^\dagger(x') r_s(x') + l_s^\dagger(x') l_s(x') - \chi_s^\dagger(x') \chi_s(x')]} \end{aligned} \quad (89)$$

Here the second term is the contribution of the string arising from the upper boundary of integration x . By virtue of the presence of the strongly oscillatory factor e^{iqx} in the expression (80) for the spectral function, the leading contribution to the spectral function arises from the part of $\mathcal{O}_s(x)$ proportional to e^{-iqx} :

$$\mathcal{O}_s(x) = \mathcal{O}_s^{(q)}(x) e^{-iqx} + \dots \quad (90)$$

In terms of this component, we have

$$\begin{aligned} A_<(\omega, k_F - q) &\sim -i \int_0^\infty dt \int_{-\infty}^\infty dx e^{i\omega t} \langle \mathcal{O}_c^\dagger(0, 0) \mathcal{O}_c(t, x) \rangle \\ &\quad \times \langle \mathcal{O}_s^{(q)\dagger}(0, 0) \mathcal{O}_s(t, x) \rangle. \end{aligned} \quad (91)$$

In order to isolate the desired contribution, we expand the second factor in Eq. (89):

$$\begin{aligned} \mathcal{O}_s^{(q)}(x) &\sim e^{-iqx} \left\{ r_s(x) \left[\frac{\pi}{2q} r_s^\dagger(x) \chi_s^\dagger(x) + \dots \right] \right. \\ &\quad \left. + \chi_s^\dagger(x) \left[1 - \frac{\pi^2}{8q^2} \{ \chi_s(x) r_s(x), r_s^\dagger(x) \chi_s^\dagger(x) \} + \dots \right] \right\} \\ &\quad \times e^{-\frac{i\pi}{2} \int_{-\infty}^x dx' [r_s^\dagger(x') r_s(x') + l_s^\dagger(x') l_s(x') - \chi_s^\dagger(x') \chi_s(x')]} \end{aligned} \quad (92)$$

In order to proceed further, it is convenient to bosonize the low-energy degrees of freedom associated with r_s , l_s using (68):

$$\begin{aligned} \mathcal{O}_s^{(q)}(x) &\sim e^{-iqx} \chi_s^\dagger(x) [b_0 + b_1 \partial_x \varphi_s^*(x) + \dots] \\ &\quad \times e^{\frac{i\pi}{4\sqrt{2}} \Phi_s^*(x) + \frac{i\pi}{2} \int_{-\infty}^x dx' \chi_s^\dagger(x') \chi_s(x')}. \end{aligned} \quad (93)$$

This can be simplified further using the appropriate operator product expansions. In order to determine the threshold

singularity, it is sufficient to retain only the term with the lowest scaling dimension at low energies, which is

$$\mathcal{O}_s^{(q)}(t, x) \sim e^{-iqx} \chi_s^\dagger(t, x) e^{\frac{i}{4\sqrt{2}} \Phi_s^*(t, x)}. \quad (94)$$

The two-point correlator of this operator is

$$\begin{aligned} & \langle \mathcal{O}_s^{(q)\dagger}(0, 0) \mathcal{O}_s^{(q)}(t, x) \rangle \\ & \sim e^{-iqx} (x^2 - v_s'^2 t^2)^{-\frac{1}{16}} e^{i\varepsilon_s t} \frac{\sin[\Lambda''(x - u_s t)]}{\pi(x - u_s t)}. \end{aligned} \quad (95)$$

Sending the cutoff Λ'' to infinity turns the last term into a delta function $\delta(x - u_s t)$. Substituting the resulting expression for (95) and the charge sector contribution (84) into the expression (80) for the hole spectral function and then carrying out the space and time integrals, we arrive at the following result for the threshold behavior:

$$A_<(\omega, k_F - q) \propto |\omega + \varepsilon_s|^{-1/4}. \quad (96)$$

As expected there is a threshold singularity. The exponent is seen to be momentum independent. As we will see, this is particular to the LE point.

V. MOBILE IMPURITY MODEL AWAY FROM THE LE POINT

We now wish to generalize the above analysis to the Luttinger liquid phase surrounding the LE point. We will assume that

1. the spinon mass term is fine-tuned to zero, i.e. $g_{s,1} = 0$;
2. the four fermion interactions in the spin and charge sectors are *attractive*, i.e., $g_{c,0}, g_{s,0} < 0$, and sizable.

Under these assumptions holons and spinons remain gapless, and the g_1 term in Eq. (72) is irrelevant so that we can drop it at low energies. Focussing again on the single-electron spectral function, using the decomposition (85), and finally, bosonizing the low-energy spin and charge degrees of freedom, we arrive at a mobile impurity model of the form

$$\mathcal{H}_{\text{MIM}} = \int dx \left[\sum_{\alpha=c,s} \mathcal{H}_\alpha + \mathcal{H}_{\text{imp}} + \mathcal{H}_{\text{int}} \right], \quad (97)$$

$$\begin{aligned} \mathcal{H}_\alpha &= \frac{v_\alpha}{16\pi} \left[\frac{1}{2K_\alpha} (\partial_x \Phi_\alpha^*)^2 + 2K_\alpha (\partial_x \Theta_\alpha^*)^2 \right], \\ \mathcal{H}_{\text{imp}} &= \chi_s^\dagger (\varepsilon_s - i u_s \partial_x) \chi_s, \end{aligned} \quad (98)$$

$$\mathcal{H}_{\text{int}} = \chi_s^\dagger \chi_s \left[\sum_\alpha f_\alpha(q) \partial_x \varphi_\alpha^* + \bar{f}_\alpha(q) \partial_x \bar{\varphi}_\alpha^* \right].$$

Here, we have dropped all terms that do not affect the threshold exponent and retained the same parametrization of the impurity part of the Hamiltonian, although the actual values of ε_s and u_s are of course not the same as the LE point. The Luttinger parameter in the spin sector varies from $K_s = 1/2$ at the LE point to $K_s = 1$ in the SU(2)-invariant limit. The charge Luttinger parameter equals $K_c = 1/2$ at the LE point, and varies with doping and interaction strength otherwise. We note that close to the LE point (in the sense that $g_{c,0}, g_{s,0}$ are small), there is an additional contribution to \mathcal{H}_{int} of the form $\chi_s^\dagger \chi_s \cos(\Phi_s^*/\sqrt{2})$. The analysis of this case is very interesting (see, e.g., Ref. [68] for a related problem), but beyond the

scope of our work. The functions $f_\alpha(q)$, $\bar{f}_\alpha(q)$ as well as the parameters v_α , K_α , ε_s , u_s depend on the microscopic details of the particular lattice realization of our field theory. We will show below how they can be fixed either numerically in the generic case or analytically when our theory is applied to the Hubbard model.

The mobile impurity model (98) can now be analyzed by standard methods [54,60]. The interaction between the impurity and the low-energy degrees of freedom can be removed through a unitary transformation

$$U = e^{-i \int_{-\infty}^{\infty} dx \sum_\alpha [\gamma_\alpha \varphi_\alpha^*(x) + \bar{\gamma}_\alpha \bar{\varphi}_\alpha^*(x)] \chi_s^\dagger(x) \chi_s(x)}. \quad (99)$$

The transformed spin impurity field equals

$$\begin{aligned} d_s(x) &= U \chi_s(x) U^\dagger \\ &= \chi_s(x) e^{i \sum_\alpha [\gamma_\alpha \varphi_\alpha^*(x) + \bar{\gamma}_\alpha \bar{\varphi}_\alpha^*(x)]} e^{-i\pi \sum_\alpha (\gamma_\alpha^2 - \bar{\gamma}_\alpha^2) C(x)}, \end{aligned} \quad (100)$$

while the chiral spin and charge Bose fields transform as

$$\begin{aligned} \varphi_\alpha^\circ(x) &= U \varphi_\alpha^*(x) U^\dagger = \varphi_\alpha^*(x) - 2\pi \gamma_\alpha C(x), \\ \bar{\varphi}_\alpha^\circ(x) &= U \bar{\varphi}_\alpha^*(x) U^\dagger = \bar{\varphi}_\alpha^*(x) + 2\pi \bar{\gamma}_\alpha C(x), \end{aligned} \quad (101)$$

where

$$C(x) = \int_{-\infty}^{\infty} dy \operatorname{sgn}(x - y) \chi_s^\dagger(y) \chi_s(y). \quad (102)$$

We note that

$$\begin{aligned} \partial_x \varphi_\alpha^\circ(x) &= \partial_x \varphi_\alpha^*(x) - 4\pi \gamma_\alpha \chi_s^\dagger(x) \chi_s(x), \\ \partial_x \bar{\varphi}_\alpha^\circ(x) &= \partial_x \bar{\varphi}_\alpha^*(x) + 4\pi \bar{\gamma}_\alpha \chi_s^\dagger(x) \chi_s(x). \end{aligned} \quad (103)$$

Adjusting the parameters γ_α , $\bar{\gamma}_\alpha$ such that

$$\begin{pmatrix} f_\alpha \\ \bar{f}_\alpha \end{pmatrix} = \begin{pmatrix} u - v_\alpha^+ & -v_\alpha^- \\ v_\alpha^- & v_\alpha^+ + u \end{pmatrix} \begin{pmatrix} \gamma_\alpha \\ \bar{\gamma}_\alpha \end{pmatrix}, \quad (104)$$

with

$$v_\alpha^\pm = \frac{v_\alpha}{2} \left(2K_\alpha \pm \frac{1}{2K_\alpha} \right), \quad (105)$$

the impurity decouples in the new variables:

$$\begin{aligned} \mathcal{H}_{\text{MIM}} &= \int dx \left(\sum_{\alpha=c,s} \mathcal{H}'_\alpha + \mathcal{H}'_{\text{imp}} \right), \\ \mathcal{H}'_\alpha &= \frac{v_\alpha}{16\pi} \left[\frac{1}{2K_\alpha} (\partial_x \Phi_\alpha^\circ)^2 + 2K_\alpha (\partial_x \Theta_\alpha^\circ)^2 \right], \\ \mathcal{H}'_{\text{imp}} &= d_s^\dagger (\varepsilon_s - i u_s \partial_x) d_s. \end{aligned} \quad (106)$$

The interaction between the mobile impurity and the Luttinger liquid degrees of freedom is now encoded in the boundary conditions of the transformed Bose fields Φ_α° , Θ_α° , which are ‘‘twisted’’ by the presence of the impurity, see, e.g., (103). The negative-frequency part of the single-electron spectral function is again given by (91), where

$$\mathcal{O}_c(x) \mathcal{O}_s^{(q)}(x) \sim e^{-iqx} \chi_s^\dagger e^{\frac{i}{4\sqrt{2}} \Phi_s^*} e^{-\frac{i}{\sqrt{2}} \varphi_c^*} e^{\frac{i}{4\sqrt{2}} \Phi_c^*}. \quad (107)$$

In terms of the transformed fields, this reads

$$\begin{aligned} \mathcal{O}_c(x) \mathcal{O}_s^{(q)}(x) &\sim e^{-iqx} d_s^\dagger e^{i(\gamma_s + \frac{1}{4\sqrt{2}}) \varphi_s^\circ + i(\bar{\gamma}_s + \frac{1}{4\sqrt{2}}) \bar{\varphi}_s^\circ} \\ &\quad \times e^{i(\gamma_c - \frac{3}{4\sqrt{2}}) \varphi_c^\circ + i(\bar{\gamma}_c + \frac{1}{4\sqrt{2}}) \bar{\varphi}_c^\circ}. \end{aligned} \quad (108)$$

The threshold behavior of the hole spectral function can now be calculated in the same way as at the LE point. The result is

$$A_{<}(\omega, k_F - q) \sim \frac{1}{|\omega + \epsilon_0|^\mu}, \quad (109)$$

where the exponent μ is given by

$$\begin{aligned} \mu &= 1 - 2(v_{c,+}^2 + v_{c,-}^2 + v_{s,+}^2 + v_{s,-}^2), \\ v_{c,\pm} &= \sqrt{\frac{K_c}{2}} \left(\gamma_c + \bar{\gamma}_c - \frac{1}{2\sqrt{2}} \right) \pm \frac{1}{\sqrt{8K_c}} \left(\gamma_c - \bar{\gamma}_c - \frac{1}{\sqrt{2}} \right), \\ v_{s,\pm} &= \sqrt{\frac{K_s}{2}} \left(\gamma_s + \bar{\gamma}_s + \frac{1}{2\sqrt{2}} \right) \pm \frac{1}{\sqrt{8K_s}} (\gamma_s - \bar{\gamma}_s). \end{aligned} \quad (110)$$

As $\gamma_\alpha, \bar{\gamma}_\alpha$ are functions of q , the threshold exponent is now generally momentum dependent. However, it is shown in Appendix C that spin rotational SU(2) symmetry in the limit $K_s \rightarrow 1$ enforces the particular values

$$\gamma_s = \bar{\gamma}_s = -\frac{1}{4\sqrt{2}}, \quad (111)$$

for any value of q .

A. Relation of $\gamma_\alpha, \bar{\gamma}_\alpha$ to finite-size energy spectra

An obvious question is whether there is a way of directly determining the parameters $\gamma_\alpha, \bar{\gamma}_\alpha$ for a given microscopic lattice model. To that end, let us consider the spectrum of our mobile impurity model on a large, finite ring of circumference L . The mode expansions of the Bose fields $\varphi_\alpha^*, \bar{\varphi}_\alpha^*$ are

$$\begin{aligned} \varphi_\alpha^*(x) &= \varphi_{\alpha,0}^* + \frac{x}{L} Q_\alpha^* + \sum_{n=1}^{\infty} \sqrt{\frac{2}{n}} \left(e^{i\frac{2\pi n}{L}x} a_{\alpha,R,n} + e^{-i\frac{2\pi n}{L}x} a_{\alpha,R,n}^\dagger \right), \\ \bar{\varphi}_\alpha^*(x) &= \bar{\varphi}_{\alpha,0}^* + \frac{x}{L} \bar{Q}_\alpha^* + \sum_{n=1}^{\infty} \sqrt{\frac{2}{n}} \left(e^{-i\frac{2\pi n}{L}x} a_{\alpha,L,n} + e^{i\frac{2\pi n}{L}x} a_{\alpha,L,n}^\dagger \right). \end{aligned} \quad (112)$$

Here, $Q_\alpha^*, \bar{Q}_\alpha^*, \varphi_{\alpha,0}^*$, and $\bar{\varphi}_{\alpha,0}^*$ are zero mode operators with commutation relations

$$[\varphi_{\alpha,0}^*, Q_\alpha^*] = -4\pi i = -[\bar{\varphi}_{\alpha,0}^*, \bar{Q}_\alpha^*]. \quad (113)$$

The eigenvalues q_α, \bar{q}_α of the zero mode operators $Q_\alpha^*, \bar{Q}_\alpha^*$ depend on the boundary conditions on the fields $\varphi_\alpha^*, \bar{\varphi}_\alpha^*$, which on general grounds will depend on whether or not a mobile impurity is present. In the presence of the impurity, the finite-size spectrum of (98) has the following structure:

$$E = E_{\text{GS}} + E_{\text{imp}} + \Delta E_{\text{LL}} + o(L^{-1}). \quad (114)$$

Here, E_{imp} is the contribution of the impurity to the energy. On general grounds, it will have the following expansion in terms of the system size:

$$E_{\text{imp}} = E_{\text{imp}}^{(0)} + \frac{1}{L} E_{\text{imp}}^{(1)} + o(L^{-1}). \quad (115)$$

The other contribution to (114) arises from the Luttinger-liquid part of the theory. Applying the mode expansions to the

transformed Hamiltonian (106), we obtain

$$\begin{aligned} \Delta E_{\text{LL}} &= \sum_{\alpha=c,s} \frac{2\pi v_\alpha}{L} \left[\frac{1}{4K_\alpha} \left(\frac{q_\alpha + \bar{q}_\alpha}{4\pi} - \gamma_\alpha + \bar{\gamma}_\alpha \right)^2 \right. \\ &\quad \left. + K_\alpha \left(\frac{q_\alpha - \bar{q}_\alpha}{4\pi} - \gamma_\alpha - \bar{\gamma}_\alpha \right)^2 + \sum_{n>0} n [M_{n,\alpha}^+ + M_{n,\alpha}^-] \right]. \end{aligned} \quad (116)$$

Here, q_α, \bar{q}_α , and $M_{n,\alpha}^\pm$ are “quantum numbers” characterizing a particular low-energy excitation. Their quantization conditions depend on the boundary conditions for the spin and charge Bose fields (112) in the presence of a high-energy mobile impurity. These can be worked out by considering the “minimal” excitation that can be made in the sector where the mobile impurity is present. This sector is reached by acting with the operator

$$\mathcal{O}_c(x) \mathcal{O}_s^{(q)}(x) = e^{-iqx} \chi_s^\dagger e^{\frac{i}{4\sqrt{2}} \Phi_s^\circ} e^{-\frac{i}{\sqrt{2}} \varphi_c^\circ} e^{\frac{i}{4\sqrt{2}} \Phi_c^\circ} \quad (117)$$

on the ground state $|\psi_0\rangle$. The latter is characterized by being annihilated by $a_{\alpha,R,n}, a_{\alpha,L,n}, Q_\alpha^*$, and \bar{Q}_α^* . The quantum numbers of the “minimal” excitation are found by noting that

$$\begin{aligned} Q_\alpha^* \mathcal{O}_c(x) \mathcal{O}_s^{(q)}(x) |\psi_0\rangle &= [Q_\alpha^*, \mathcal{O}_c(x) \mathcal{O}_s^{(q)}(x)] |\psi_0\rangle \\ &= q_\alpha^{(0)} \mathcal{O}_c(x) \mathcal{O}_s^{(q)}(x) |\psi_0\rangle, \end{aligned} \quad (118)$$

where

$$q_c^{(0)} = \frac{3\pi}{\sqrt{2}}, \quad \bar{q}_c^{(0)} = \frac{\pi}{\sqrt{2}}, \quad q_s^{(0)} = -\bar{q}_s^{(0)} = -\frac{\pi}{\sqrt{2}}. \quad (119)$$

Let us denote the lowest-energy state with these quantum numbers by

$$|q_c^{(0)}, \bar{q}_c^{(0)}, q_s^{(0)}, \bar{q}_s^{(0)}\rangle. \quad (120)$$

Higher excited states in the “impurity sector” can be obtained, for example, by making particle-hole excitations on top of the state (120). The energies of such states are given by (116) by choosing (119) and in addition taking some of the $M_{n,\alpha}^\pm$ different from zero. Crucially, the values of $\gamma_\alpha, \bar{\gamma}_\alpha$ are the same as for the state (120). For practical purposes, states with the same momentum as (120) but different spin and charge quantum numbers might be of particular interest as they are the lowest energy states in certain sectors of quantum numbers and can therefore be more easily targeted in DMRG computations. The quantum numbers for such states are

$$\begin{aligned} q_\alpha &= q_\alpha^{(0)} + \frac{\pi}{\sqrt{2}} (3m_\alpha + \bar{m}_\alpha), \\ \bar{q}_\alpha &= \bar{q}_\alpha^{(0)} + \frac{\pi}{\sqrt{2}} (3\bar{m}_\alpha + m_\alpha), \end{aligned} \quad (121)$$

where m_α, \bar{m}_α are integers. This follows from the mode expansion and the requirement that the bosonized expressions for $R_\uparrow(x), R_\downarrow(x), L_\uparrow(x), L_\downarrow(x)$ must be single valued. Using that at low energies, the charge, spin densities, and currents are given by

$$\begin{aligned} \rho_\alpha(x) &= -\frac{1}{\pi\sqrt{8}} \partial_x \Phi_\alpha^\circ(x), \\ j_\alpha(x) &= -\frac{1}{\pi\sqrt{8}} \partial_x \Theta_\alpha^\circ(x), \end{aligned} \quad (122)$$

we can identify that

$(m_c + \bar{m}_c)/2$ is the difference in charge (particle number) between the excitation and the state (120),

$(m_c - \bar{m}_c)/2$ is the number of charge fermions transferred from the right-moving to the left-moving branch,

$(m_s + \bar{m}_s)/2$ is the difference in the number of down spins between the excitation and the state (120),

$(m_s - \bar{m}_s)/2$ is the number of spin fermions transferred from the right-moving to the left-moving branch.

The values of $\gamma_\alpha, \bar{\gamma}_\alpha$ can now in principle be extracted by numerically computing finite-size energy levels by a method such as momentum-space DMRG [69,70]. The procedure is outlined in the following:

(1) The velocities v_α and Luttinger parameters K_α are bulk properties and can be determined by standard methods. We will assume them to be known quantities in the following. We further denote the number of particles and down spins in the ground state by N_{GS} and M_{GS} , respectively.

(2) We then numerically compute the lowest excitation with momentum q and quantum numbers $N = N_{\text{GS}} - 1$, $M = M_{\text{GS}} - 1$. Its energy is

$$E_{-1,-1} = E_{\text{GS}} + E_{\text{imp}}^{(0)} + \frac{1}{L} E_{\text{imp}}^{(1)} + \Delta E_{\text{LL}}(q_c^{(0)}, \bar{q}_c^{(0)}, q_s^{(0)}, \bar{q}_s^{(0)}) + o(L^{-1}). \quad (123)$$

(3) Next, we compute the lowest excitations with momentum q but different values of N and M . For example, choosing

$$N = N_{\text{GS}} - 1, \quad M = M_{\text{GS}} - 2, \quad (124)$$

gives the excited state characterized by

$$m_c = -\bar{m}_c = 1, \quad m_s = -2, \bar{m}_s = 0. \quad (125)$$

The zero-mode eigenvalues follow from (121)

$$\begin{aligned} q_c^{(1)} &= \frac{5\pi}{\sqrt{2}}, & \bar{q}_c^{(1)} &= -\frac{\pi}{\sqrt{2}}, \\ q_s^{(1)} &= -\frac{7\pi}{\sqrt{2}}, & \bar{q}_s^{(1)} &= -\frac{\pi}{\sqrt{2}}. \end{aligned} \quad (126)$$

The corresponding energy is

$$E_{-1,-2} = E_{\text{GS}} + E_{\text{imp}}^{(0)} + \frac{1}{L} E_{\text{imp}}^{(1)} + \Delta E_{\text{LL}}(q_c^{(1)}, \bar{q}_c^{(1)}, q_s^{(1)}, \bar{q}_s^{(1)}) + o(L^{-1}). \quad (127)$$

Here, we have asserted that the change in the impurity contribution to the energy is of higher order in L^{-1} . This has been shown for the case of the Hubbard model using methods of integrability in Ref. [53]. We believe that this continues to hold true in general, because $E_{\text{imp}}^{(1)}$ is sensitive only to the values of the parameters $\gamma_\alpha, \bar{\gamma}_\alpha$, which are the same for all excitations we are considering.

The point is that by considering energy differences like

$$\begin{aligned} E_{-1,-2} - E_{-1,-1} &= \Delta E_{\text{LL}}(q_c^{(1)}, \bar{q}_c^{(1)}, q_s^{(1)}, \bar{q}_s^{(1)}) \\ &\quad - \Delta E_{\text{LL}}(q_c^{(0)}, \bar{q}_c^{(0)}, q_s^{(0)}, \bar{q}_s^{(0)}) + o(L^{-1}) \end{aligned} \quad (128)$$

we obtain a set of equations in which the only unknown parameters are the $\gamma_\alpha, \bar{\gamma}_\alpha$. This provides a numerical method for determining them in a general lattice model. For integrable theories like the Hubbard model, analytical techniques are available and we discuss this case next.

B. Hubbard model

The finite-size spectrum in presence of a high-energy spinon excitation was calculated for the case of the Hubbard model using the Bethe ansatz solution in Ref. [53]. The result for the lowest excited state above the spinon threshold is

$$\begin{aligned} E &= E_{\text{GS}} - \epsilon_s(\Lambda^h) - \frac{1}{L} \epsilon'_s(\Lambda^h) \delta \Lambda^h \\ &\quad + \frac{2\pi v_c}{L} \left[\frac{(\Delta N_c - N_c^{\text{imp}})^2}{8K_c} + 2K_c \left(D_c - D_c^{\text{imp}} + \frac{D_s}{2} \right)^2 \right] \\ &\quad + \frac{2\pi v_s}{L} \left[\frac{(\Delta N_s - \frac{1}{2} \Delta N_c - \frac{1}{2})^2}{2} + \frac{D_s^2}{2} \right] + o(L^{-1}), \end{aligned} \quad (129)$$

where

$$D_s = D_c = 0, \quad \Delta N_c = -1, \quad \Delta N_s = 0. \quad (130)$$

The contribution $-\epsilon_s(\Lambda^h) - \frac{1}{L} \epsilon'_s(\Lambda^h) \delta \Lambda^h$ is the finite-size energy of the impurity. The velocities v_α, K_α as well as the quantities N_c^{imp} and D_c^{imp} are expressed in terms of solutions to coupled linear integral equations, and in practice are easily calculated numerically with very high precision. By construction, the quantum numbers (130) correspond to our minimal excited state (120). By matching the Luttinger liquid part of the energy to (114) we then obtain the following results for the parameters $\gamma_\alpha, \bar{\gamma}_\alpha$:

$$\begin{aligned} \gamma_c + \bar{\gamma}_c &= \frac{1}{2\sqrt{2}} - \sqrt{2} D_c^{\text{imp}}, & \gamma_c - \bar{\gamma}_c &= -\frac{N_c^{\text{imp}}}{\sqrt{2}}, \\ \gamma_s &= \bar{\gamma}_s = -\frac{1}{4\sqrt{2}}. \end{aligned} \quad (131)$$

One subtlety to keep in mind when making contact between the Bethe ansatz calculation and (114) is that the former refers only to highest weight states of the $\text{SU}(2) \otimes \text{SU}(2)$ symmetry algebra of the Hubbard model [71,72]. Descendant states need to be taken into account separately. Substituting (131) in the expressions for the quantities v_α^\pm (110), we find

$$v_s^\pm = 0, \quad v_c^\pm = -\sqrt{K_c} D_c^{\text{imp}} \mp \frac{1 + N_c^{\text{imp}}}{4\sqrt{K_c}}. \quad (132)$$

Finally, the threshold exponent is obtained from (110):

$$\mu = 1 - \frac{(1 + N_c^{\text{imp}})^2}{4K_c} - 4K_c (D_c^{\text{imp}})^2. \quad (133)$$

This agrees with what was found in Ref. [53] using the approach of Schmidt, Imambekov, and Glazman [51,52], as well as with the exponents reported previously in Refs. [31–33].

I. Other excited states

The Bethe ansatz result (129) can be applied to other excited states as well. In particular, the holon plus three spinon excitation considered in Ref. [53] gives rise to an excitation with the same momentum and quantum numbers:

$$\Delta N_c = -1 = \Delta N_s, \quad D_s = -1, \quad D_c = \frac{1}{2}. \quad (134)$$

The corresponding state in our mobile impurity model has quantum numbers (125), and the energies calculated from (114) and (129) agree as they must.

VI. RELATION TO THE APPROACH OF SCHMIDT, IMAMBEKOV AND GLAZMAN

The method of Refs. [51,52] is based on a different prescription for defining fermionic quasiparticles in the charge and spin sectors. We now summarize the main steps of this approach and compare them to our framework. The starting point is the standard bosonized description (53) of the spinful fermion model under consideration. One then introduces the chiral components $\phi_\alpha, \bar{\phi}_\alpha$ by

$$\Phi_\alpha(x) = \sqrt{K_\alpha}(\phi_\alpha + \bar{\phi}_\alpha), \quad (135)$$

$$\Theta_\alpha(x) = \frac{1}{\sqrt{K_\alpha}}(\phi_\alpha - \bar{\phi}_\alpha). \quad (136)$$

These chiral bosons diagonalize the spinful Luttinger model (53) in the form

$$\mathcal{H}_{LL}(x) = \sum_{\alpha=c,s} \frac{v_\alpha}{8\pi} [(\partial_x \phi_\alpha)^2 + (\partial_x \bar{\phi}_\alpha)^2]. \quad (137)$$

Next, in analogy with the spinless case in Eqs. (41) and (42), one defines the quasiparticle operators

$$\tilde{R}_\alpha(x) \sim e^{-\frac{i}{\sqrt{2}}\phi_\alpha(x)}, \quad \tilde{L}_\alpha(x) \sim e^{\frac{i}{\sqrt{2}}\bar{\phi}_\alpha(x)}. \quad (138)$$

As in the spinless case, this prescription removes the marginal interactions between quasiparticles, rendering them asymptotically free in the low-energy limit. However, these quasiparticles cannot be identified with the finite energy elementary excitations in integrable models, because they carry fractional quantum numbers:

$$[q_\alpha, \tilde{R}_\alpha^\dagger(x)] = \sqrt{2K_\alpha} \tilde{R}_\alpha^\dagger, \quad [q_\alpha, \tilde{L}_\alpha^\dagger(x)] = \sqrt{2K_\alpha} \tilde{L}_\alpha^\dagger. \quad (139)$$

The only exception is the LE point $K_\alpha = 1/2$, where the operators $\tilde{R}_\alpha, \tilde{L}_\alpha$ in fact carry the same quantum numbers as our spin and charge fermions.

Despite the lack of correspondence with long-lived excitations in (nearly) integrable models, the approach of Refs. [51,52] allows one to compute threshold exponents, as long as the parameters in the effective impurity model are adjusted appropriately. The situation is analogous to the two ways of determining threshold exponents discussed above in the spinless fermion case.

In order to facilitate a direct comparison with our approach, we briefly review how to express the electron operator in order to calculate the threshold exponent in the single-particle spectral function within the approach of Refs. [51,52]. We assume again that the lower threshold of the support corresponds to an excitation with a single high-energy spinon. First, the

right-moving spin quasiparticle in Eq. (138) is projected into low-energy and impurity subbands:

$$\tilde{R}_s(x) \sim \tilde{r}_s(x) + e^{-iqx} \tilde{\chi}_s^\dagger(x). \quad (140)$$

One then rewrites the electron operator in terms of the quasiparticles defined in Eq. (138). As this differs from ours, cf Eq. (67), the string-operator part in the expression for the electron operator is also different:

$$R_\uparrow(x) \sim e^{-iqx} \tilde{\chi}_s^\dagger(x) e^{\frac{i}{\sqrt{2}}\phi_s} \prod_{\alpha=c,s} e^{-\frac{i}{4}(\sqrt{K_\alpha} + \frac{1}{\sqrt{K_\alpha}})\phi_\alpha} \times e^{-\frac{i}{4}(\sqrt{K_\alpha} - \frac{1}{\sqrt{K_\alpha}})\bar{\phi}_\alpha}. \quad (141)$$

The next step is to write down an effective impurity model, analogous to Eq. (98), but using $\tilde{\chi}_s$ as the impurity. After performing a unitary transformation that removes the coupling between $\tilde{\chi}_s$ and the low-energy modes, the electron operator becomes

$$R_\uparrow(x) \sim e^{-iqx} \tilde{d}_s^\dagger(x) e^{-\frac{i}{4}(\sqrt{K_s} + \frac{1}{\sqrt{K_s}} - 2\sqrt{2} - 4\gamma'_s)\phi_s} \times e^{-\frac{i}{4}[(\sqrt{K_s} - \frac{1}{\sqrt{K_s}} - 4\bar{\gamma}'_s)\bar{\phi}_s + (\sqrt{K_c} + \frac{1}{\sqrt{K_c}} - 4\gamma'_c)\phi_c]} \times e^{-\frac{i}{4}[(\sqrt{K_c} - \frac{1}{\sqrt{K_c}} - 4\bar{\gamma}'_c)\bar{\phi}_c]}, \quad (142)$$

where $\tilde{d}_s = U \tilde{\chi}_s U^\dagger$ is the free impurity field for the quasiparticle with fractional charge, and $\gamma'_\alpha, \bar{\gamma}'_\alpha$ are the parameters of the unitary transformation, which are not the same as $\gamma_\alpha, \bar{\gamma}_\alpha$ discussed in Sec. V.

At the LE point, we set $K_\alpha = 1/2$ and $\gamma'_\alpha = \bar{\gamma}'_\alpha = 0$ and Eq. (142) reduces to

$$R_\uparrow(x) \sim e^{-iqx} \tilde{d}_s^\dagger(x) e^{-\frac{i}{2}\phi_c} e^{\frac{i}{4\sqrt{2}}(\phi_s + \bar{\phi}_s + \phi_c + \bar{\phi}_c)}. \quad (143)$$

This result agrees with the refermionization in Sec. IV C, since at the LE point $\tilde{d}_\alpha = d_\alpha = \chi_\alpha$, $\phi_\alpha = \varphi_\alpha^*$, and $\bar{\phi}_\alpha = \bar{\varphi}_\alpha^*$; thus, the two approaches coincide.

Moving away from the LE point, the expressions for physical operators in terms of impurity and low-energy fields will in general be different in the two approaches. However, the results for the edge exponents are still consistent because the difference in string operators can be accommodated by the parameters of the unitary transformation and by imposing proper boundary conditions on the bosonic fields. For instance, imposing SU(2) symmetry in the approach of Refs. [51,52] leads to the requirements

$$\gamma'_s = \sqrt{2} - 1, \quad \bar{\gamma}'_s = 0. \quad (144)$$

This should be contrasted with Eq. (111).

VII. REALIZING THE LE POINT

We have seen that a good starting point for understanding threshold singularities in dynamical response functions is the LE point for both charge and spin. In Sec. IV, we considered properties of the LE point in the field theory limit. An obvious question raised by these considerations is whether it is possible to realize the LE point in practice in a lattice model of interacting spinful fermions. We now investigate this issue in some detail and present a number of preliminary results.

A. Lattice model

As discussed in Sec. IV A, realizing the LE point at sufficiently low energies in an extended Hubbard model of the kind (47) requires the fine-tuning of (at least) four parameters:

$$K_c = K_s = \frac{1}{2}, \quad g_{s,1} = g_1 = 0. \quad (145)$$

For the Hubbard model in zero magnetic field, spin rotational symmetry fixes $K_s = 1$, while K_c varies with both band filling and interaction strength U . In particular, it is well known [23,24] that $K_c = \frac{1}{2}$ is obtained in the $U \rightarrow \infty$ limit of the Hubbard model [14,73]. Values $K_s < 1$ can be realized by adding spin-dependent interactions that break the spin SU(2) symmetry, but retain spin inversion symmetry. The latter is crucial for avoiding marginal interactions between spin and charge sectors that lead to a more complicated conformal spectrum involving a dressed charge matrix [7,23,24].

A minimal lattice model that may allow us to fulfill the conditions in Eq. (145) is

$$H = -t \sum_{j=1}^{L-1} \sum_{\sigma} (c_{j,\sigma}^{\dagger} c_{j+1,\sigma} + \text{H.c.}) + U \sum_{j=1}^L n_{j,\uparrow} n_{j,\downarrow} + \sum_{r=1}^2 V_r \sum_{j=1}^{L-r} n_j n_{j+r} + J_1^z \sum_{j=1}^{L-1} S_j^z S_{j+1}^z. \quad (146)$$

In anticipation of the DMRG computations of energy levels reported below we have imposed open boundary conditions. In the following we set $t = 1$, i.e., measure all energies in units of the hopping parameter. The idea is then to try to adjust the four interaction strengths U , $V_{1,2}$ and J_1^z in such a way that (145) are achieved. In order to ascertain the low-energy properties of (146), we compute the energies of the ground state and several low-lying excited states for a quarter-filled band, and compare the results to expectations based on Luttinger liquid theory. We choose to work at quarter filling in order to simplify finite-size scaling analyses. As alluded to in Appendix A, working at commensurate fillings induces additional Umklapp interactions. In the case at hand, this corresponds to the presence of an additional perturbation $\int dx \cos(2\Phi_c)$. However, this term has a scaling dimension $8K_c$ and is therefore highly irrelevant for $K_c \geq 1/2$. We therefore discard it in the following analysis.

Some insight into how the parameters K_c, K_s and $g_{s,1}$ depend on U , $V_{1,2}$ and J_1^z can be gained by bosonizing the interactions at weak coupling. Using (48), we obtain in leading order

$$n_{j,\uparrow} n_{j,\downarrow} \sim \frac{\mathcal{A}}{4} [\mathcal{O}_4^{(2)}(x) + 2\mathcal{O}_5^{(2)}(x) - \mathcal{O}_2^{(2)}(x) - 2\mathcal{O}_3^{(2)}(x) + 8\eta_{\uparrow} \bar{\eta}_{\downarrow} \eta_{\downarrow} \bar{\eta}_{\uparrow} \mathcal{O}_1^{(2)}(x)], \quad (147)$$

$$n_j n_{j+1} \sim \mathcal{A} [\mathcal{O}_4^{(2)}(x) + 2\mathcal{O}_5^{(2)}(x)], \quad (148)$$

$$n_j n_{j+2} \sim \frac{\mathcal{A}}{2} [3\mathcal{O}_4^{(2)}(x) + 6\mathcal{O}_5^{(2)}(x) + \mathcal{O}_2^{(2)}(x) + 2\mathcal{O}_3^{(2)}(x) - 8\eta_{\uparrow} \bar{\eta}_{\downarrow} \eta_{\downarrow} \bar{\eta}_{\uparrow} \mathcal{O}_1^{(2)}(x)], \quad (149)$$

$$S_j^z S_{j+1}^z \sim \frac{\mathcal{A}}{4} [\mathcal{O}_2^{(2)}(x) + 2\mathcal{O}_3^{(2)}(x)]. \quad (150)$$

Here, $x = ja_0$, \mathcal{A} is a dimensionful amplitude, and

$$\begin{aligned} \mathcal{O}_1^{(2)} &= \cos \Phi_s, \\ \mathcal{O}_2^{(2)} &= (\partial_x \varphi_s)^2 + (\partial_x \bar{\varphi}_s)^2, \\ \mathcal{O}_3^{(2)} &= \partial_x \varphi_s \partial_x \bar{\varphi}_s, \\ \mathcal{O}_4^{(2)} &= (\partial_x \varphi_c)^2 + (\partial_x \bar{\varphi}_c)^2, \\ \mathcal{O}_5^{(2)} &= \partial_x \varphi_s \partial_x \bar{\varphi}_s. \end{aligned} \quad (151)$$

At weak coupling, the spin-charge separated Luttinger liquid at low energies is therefore perturbed by

$$\delta\mathcal{H} = \sum_{j=1}^5 \nu_j \int dx \mathcal{O}_j^{(2)}(x) \equiv \sum_{j=1}^5 \delta\mathcal{H}_j, \quad (152)$$

where the ν_j are proportional to linear combinations of U , V_1 , V_2 , and J_1^z . The effects of $\delta\mathcal{H}_2$ and $\delta\mathcal{H}_4$ are to renormalize the spin and charge velocities respectively, while $\delta\mathcal{H}_3$ and $\delta\mathcal{H}_5$ change the values of the Luttinger parameters K_s and K_c . We must pay special attention to the perturbation $\delta\mathcal{H}_1$: as discussed in Appendix B, this operator is marginal at weak coupling, but gives rise to the relevant spinon mass term as we approach the LE point. Our objective is to adjust U , V_1 , V_2 , and J_1^z in such a way that $K_{c,s}$ are reduced towards $1/2$, while the coupling ν_1 of the spinon mass term remains very small. The bosonization results (150) suggest the following prescription for achieving this at weak coupling: (1) increase V_2 in order to make $|\nu_1|$ very small. (2) Then adjust V_1 and J_1^z in order to drive $K_{c,s}$ towards $1/2$. Importantly, the bosonization results (150) indicate that at least at weak coupling this does not produce sizable contributions to $\delta\mathcal{H}_1$. Our analysis below is guided by these considerations, even though we are not operating in the weak coupling regime, in which (150) are applicable.

B. Finite-size spectrum of unperturbed Luttinger liquid with open boundary conditions

A standard procedure for determining the Luttinger parameters K_c and K_s is to compare the finite-size spectrum predicted by Luttinger liquid theory with the low-energy spectrum calculated numerically for a given lattice model. The finite-size spectrum relative to the ground state of a Luttinger liquid with open boundaries is given by

$$\begin{aligned} \Delta E(S^z, \Delta N_c, \{m_{\ell}^c, m_{\ell}^s\}) &= \frac{\pi v_s (S^z)^2}{K_s L} + \frac{\pi v_c (\Delta N_c)^2}{4K_c L} \\ &\quad - \frac{\pi v_c d \Delta N_c}{2K_c L} + \sum_{\alpha=c,s} \sum_{\ell=1}^{\infty} \frac{\pi v_{\alpha}}{L} \ell m_{\ell}^{\alpha} + o(L^{-1}). \end{aligned} \quad (153)$$

Here, S^z and ΔN_c are quantum numbers in the spin and charge sectors, respectively, associated with the global $U(1) \otimes U(1)$ symmetry. The value of S^z measures the change in the total magnetization and $\Delta N_c = N - N_0$ measures the change in the total number of electrons with respect to a singlet ground state with N_0 electrons. As usual, the values of S^z and ΔN_c are constrained by the selection rule that $2S^z$ must be even

(odd) if ΔN_c is even (odd). The parameter d in Eq. (153) is a dimensionless constant that depends on the definition of the chemical potential to order $1/L$. The parameters m_ℓ^s and m_ℓ^c are non-negative integers that count the number of low-energy particle-hole pairs in each sector. We note that for open boundary conditions the total momentum is not conserved and there are no quantum numbers associated with current excitations (i.e. with transferring particles between Fermi points). Thus (153) should not be confused with the spectrum in Eq. (116), which is valid for periodic boundary conditions.

The spin and charge velocities v_s and v_c can be extracted by matching the energies of the lowest excitations with $S^z = \Delta N_c = 0$. Assuming $v_s < v_c$ (which can be verified by analyzing excitations with different quantum numbers), the first excited state corresponds to $m_1^s = 1$ and has energy

$$\Delta E(0,0, \{m_\ell^s = \delta_{\ell,1}, m_\ell^c = 0\}) = \frac{\pi v_s}{L}. \quad (154)$$

Likewise, if $v_s < v_c < 2v_s$, the second excited state corresponds to $m_1^c = 1$ and has energy

$$\Delta E(0,0, \{m_\ell^s = 0, m_\ell^c = \delta_{\ell,1}\}) = \frac{\pi v_c}{L}. \quad (155)$$

Having determined the velocities, one can obtain the Luttinger parameters by analyzing low-lying excitations that change the quantum numbers S^z and ΔN_c . We adopt the short-hand notations

$$\Delta E_0(S^z, \Delta N_c) \equiv \Delta E(S^z, \Delta N_c, \{m_\ell^c = m_\ell^s = 0 \forall \ell\}) \quad (156)$$

for the lowest energies in each sector of fixed S^z and ΔN_c . To isolate the dependence on K_c , we consider excitations with $\Delta N_c = \pm 2$ and $S^z = 0$. The dependence on the unknown constant d can be eliminated by taking the combination

$$\frac{L}{4}[\Delta E_0(0,2) + \Delta E_0(0,-2)] \simeq \frac{\pi v_c}{2K_c} = \kappa^{-1}, \quad (157)$$

where we recognize κ as the compressibility of the Luttinger liquid [27]. Analogously, K_s can be determined using the relation for the finite-size spin gap

$$\frac{L}{2}\Delta E_0(1,0) = \frac{\pi v_s}{2K_s}. \quad (158)$$

The right-hand side of Eq. (158) is equal to the inverse spin susceptibility.

The procedure described above is standard for Luttinger liquids that are only perturbed by (strongly) irrelevant operators. In our case, however, we must consider the effects of the *relevant* operator $\cos \Phi_s$, which generates the spinon mass, as well as the interaction $\partial_x \Phi_c \cos \Phi_s$, which is marginal at the LE point and only weakly irrelevant in its vicinity. These perturbations introduce corrections to (154), (155), (157), and (158), which affect the finite-size scaling analysis. Since $\cos \Phi_s$ is the leading perturbation, we first focus our efforts on fine tuning it to zero, as we discuss in the next section.

C. Fine tuning the spinon mass

As anticipated in Sec. VII A, our strategy for fine tuning the spinon mass to zero starts by suppressing the coupling constant of the perturbation $\delta \mathcal{H}_1$. According to (149), for fixed

$U > 0$, this can be done efficiently by increasing the next-nearest-neighbor interaction $V_2 > 0$. In this process, we keep $V_1 = J_1^z = 0$, so the SU(2) symmetry is preserved. As we keep increasing V_2 , the marginal coupling constant will change sign at some critical value V_2^c . Beyond this point the perturbation becomes marginally relevant and the system undergoes a Berezinskii-Kosterlitz-Thouless (BKT) transition to a spin-gapped phase, analogous to the dimerization transition in the $J_1 - J_2$ spin chain [74].

Because of the exponentially small value of the gap in the vicinity of the critical point, it is difficult to pinpoint V_2^c by means of a gap scaling analysis. A better approach is to determine the critical point by searching for a level crossing in the spin excitation spectrum in the neutral sector $S^z = \Delta N_c = 0$ [75]. The idea is that in a Luttinger liquid the state with $m_2^s = 1$ should be degenerate with the state $m_1^s = 2$; however, in practice the degeneracy is lifted at order $(L \ln L)^{-1}$ due to the marginal perturbation. Exactly at the critical point, the coupling constant for $\cos(\Phi_s)$ vanishes, and V_2^c can be identified from the level crossing between $m_2^s = 1$ and $m_1^s = 2$ states.

D. Analysis of finite-size excitation energies

After tuning the coupling constant of $\delta \mathcal{H}_1$ to zero, we proceed to adjusting V_1 , and J_1^z in order to achieve values $K_{c,s} \approx \frac{1}{2}$. This has to be done while making sure that the coupling constant $g_{s,1}$ in Eq. (65), or equivalently λ_1 in Eq. (54), is held at zero as we approach the LE point. To determine the values of $K_{c,s}$, and also to ascertain that we remain in the Luttinger liquid phase as we vary the parameters of the lattice model, we resort to an analysis of the finite size energy levels of the ground state and low-lying excitations. For this purpose, we now refine the expressions presented in Sec. VII B by including the effects of the leading perturbations in the vicinity of the LE point.

An inherent difficulty encountered when approaching the LE point is that corrections to the Luttinger liquid form (153) of the finite-size energy spectrum become increasingly complicated. To see this, let us consider the bosonized form (52) of our Hamiltonian. In the regime $\frac{1}{2} < K_{s,c} < 1$, we expect the structure of the energy difference $\Delta E_0(S^z, 0)$ to be of the form

$$\begin{aligned} \Delta E_0(S^z, 0) = & \frac{a_1}{\tilde{L}^{2K_s-1}} + \frac{\pi v_s (S^z)^2}{K_s \tilde{L}} + \frac{b_1}{\tilde{L}^{2K_s}} \\ & + \frac{b_2}{\tilde{L}^{4K_s-1}} + \frac{b_3}{\tilde{L}^{6K_s-2}} + \dots, \end{aligned} \quad (159)$$

where we have defined $\tilde{L} = L + 1$. The origin of the various contributions is as follows: (1) The a_1 term arises from first order perturbation theory in the spinon mass term $\lambda_1 \int dx \cos \Phi_s$. As a consequence of our fine-tuning we expect a_1 to be quite small, so that higher orders of perturbation theory can be neglected. (2) The b_1 term arises from first-order perturbation theory in $\lambda_2 \int dx \partial_x \Phi_c \cos \Phi_s$ (which generally is nonzero for open boundary conditions). (3) The b_2 and b_3 terms arise from second- and third-order perturbation theory in $\lambda_2 \int dx \partial_x \Phi_c \cos \Phi_s$, respectively. Here we need to consider higher orders in perturbation theory because the

bare λ_2 has not been fine tuned and is not guaranteed to be small.

We see that the size dependence becomes increasingly complex as K_s tends towards $1/2$, which complicates the analysis of energy levels. A good way of achieving an accurate description of finite-size energies would be through (two-loop) renormalization-group-improved perturbation theory around both the LE point and the weak-coupling limits. However, as this is quite involved, we content ourselves with the simpler form (159) (and stress again that our numerical analysis is to be considered as preliminary).

1. Determining the Luttinger parameter K_s

Equation (159) provides us with an alternative way of determining K_s by considering the system-size dependence of the quantity

$$\delta(L) \equiv \frac{1}{4} \Delta E_0(2,0) - \Delta E_0(1,0). \quad (160)$$

Using the expression (159), we obtain

$$\delta(L) = \frac{\tilde{a}_1}{\tilde{L}^{2K_s-1}} + \frac{\tilde{b}_1}{\tilde{L}^{2K_s}} + \frac{\tilde{b}_2}{\tilde{L}^{4K_s-1}} + \dots \quad (161)$$

By fitting $\delta(L)$ computed numerically for a range of system sizes to (161), we obtain a value for K_s .

2. Determining the spin velocity v_s

Given K_s , we may determine v_s from the size dependence in Eq. (159). Alternatively we can consider other excited states, whose finite-size energies can be analyzed similarly. For example, for $v_s < v_c$, the size dependence of the first excited state in the neutral sector is given by

$$\begin{aligned} \Delta E(0,0, \{m_\ell^s = \delta_{\ell,1}, m_\ell^c = 0\}) \\ = \frac{\tilde{a}_1^s}{\tilde{L}^{2K_s-1}} + \frac{\pi v_s}{\tilde{L}} + \frac{\tilde{b}_1^s}{\tilde{L}^{2K_s}} + \frac{\tilde{b}_2^s}{\tilde{L}^{4K_s-1}} + \dots \end{aligned} \quad (162)$$

By computing the energy difference (162) numerically for a range of system sizes, using \tilde{a}_1^s and $\tilde{b}_{1,2}^s$ as fit parameters, and fixing K_s to be the value obtained from the analysis of $\delta(L)$ in Eq. (161), we may extract the spin velocity v_s .

3. Determining the charge velocity v_c

The structure of finite-size corrections to energy levels of charge excitations is somewhat simpler because some of the terms in first-order perturbation theory vanish. For $v_s < v_c < 2v_s$, the energy of the second excited state in the neutral sector scales as

$$\begin{aligned} \Delta E(0,0, \{m_\ell^s = 0, m_\ell^c = \delta_{\ell,1}\}) \\ = \frac{\pi v_c}{\tilde{L}} + \frac{\tilde{b}_2^c}{\tilde{L}^{4K_s-1}} + \dots \end{aligned} \quad (163)$$

Using the results for K_s from the analysis described in Sec. VIID1, Eq. (163) provides us with a means of determining v_c through a finite-size scaling analysis.

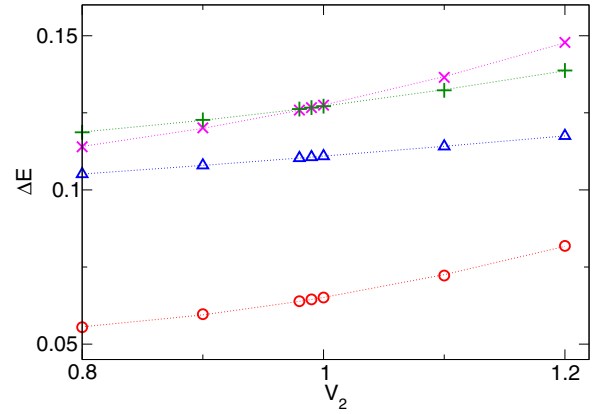


FIG. 3. (Color online) Energies of the four lowest excited states in the neutral sector $S^z = \Delta N_c = 0$ for $U = 3$, $J_1^z = V_1 = 0$, and $L = 64$ as a function of V_2 . The critical value V_2^c is identified through the crossing of the two nearly degenerate states in the $(2s, 0)$ multiplet. Lines are guide to the eye.

4. Determining K_c

Finally, the energy difference related to the compressibility (157) is found to have the following size dependence:

$$\begin{aligned} \frac{\Delta E_0(0,2) + \Delta E_0(0,-2)}{16} &= \frac{\pi v_c}{8K_c \tilde{L}} + \frac{b_2^c}{\tilde{L}^{4K_s-1}} + \dots \\ &\equiv f(L). \end{aligned} \quad (164)$$

We can use (164) together with K_s and v_c determined in Secs. VIID1 and VIID3, respectively, to fix the Luttinger parameter K_c through a finite-size scaling analysis of $f(L)$, taking b_2^c to be a fit parameter.

E. Numerical results

We now turn to the numerical implementation of the method set out in the previous subsection. We performed DMRG [76,77] computations on lattices with up to $L = 216$ sites, keeping up to 3000 states and running up to 36 finite-size sweeps. In case of the Hubbard model we have checked the energies obtained in this way against the exact Bethe ansatz results and found the relative errors to be of order 10^{-9} .

We work with model (146) at fixed $U = 3$ and search for the LE point by varying V_1 , V_2 and J_1^z . The first step is to increase V_2 keeping $V_1 = J_1^z = 0$. In Fig. 3, we show the first four excitations in the neutral sector for $L = 64$ as a function of V_2 . By tracking the evolution of the energies starting from $V_2 = 0$, i.e., the Hubbard model, we are able to identify the quantum numbers $\{m_\ell^s, m_\ell^c\}$ for each of these states. The two nearly degenerate spin descendant states of interest correspond to the third and fourth excited states. From the crossing of these two energy levels, we estimate $V_2^c \approx 1.0$.

Next, we vary V_1 and J_1^z to bring K_c and K_s close to $1/2$. After searching in parameter space, we settle for the particular parameter set

$$U = 3, \quad V_1 = 0.85, \quad V_2 = 1.1, \quad J_1^z = 5.2. \quad (165)$$

The analysis presented below suggests that this corresponds to Luttinger parameter values of $K_s = 0.655$ and $K_c = 0.500$. This is probably as close to the LE point as one can get without

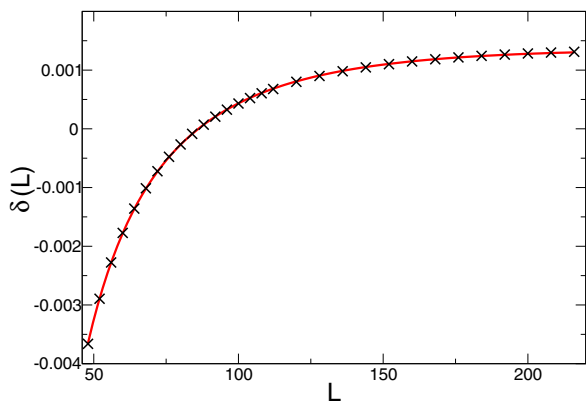


FIG. 4. (Color online) Crosses represent numerical results for $\delta(L)$ as defined in Eq. (160). The solid line is the best fit to Eq. (161) and is obtained for $K_s = 0.655$, $\tilde{a}_1 = 0.009$, $\tilde{b}_1 = 0.493$, and $\tilde{b}_2 = -5.131$.

a more precise theoretical description of finite-size energies based on a renormalization-group-improved perturbation theory analysis.

Figure 4 shows numerical results for the quantity $\delta(L)$ defined in Eq. (160). The data have been fitted using (161). The resulting best-fit estimates are

$$K_s = 0.655, \quad (166)$$

$\tilde{a}_1 = 0.009$, $\tilde{b}_1 = 0.493$, and $\tilde{b}_2 = -5.131$. The quality of the fit is visibly excellent (the residuals are $\sim 10^{-6}$). The numerical value for \tilde{a}_1 is very small, confirming that we have almost succeeded with fine-tuning the spinon mass term to zero (on the scale set by the system sizes we consider).

In the next step, we determine the spin velocity using (159) and by retaining the b_1 and b_2 terms. Setting $K_s = 0.655$, we obtain

$$v_s \approx 1.707. \quad (167)$$

This value is consistent with the result obtained by considering $\Delta E(0,0, \{m_\ell^s = \delta_{\ell,1}, m_\ell^c = 0\})$ in Eq. (162). We have verified that the energy level corresponds to the first spin descendant state by tracking the tower of lowest-lying energies in the neutral sector along a path in parameter space connecting the Hubbard model to the point (165).

Having determined v_s and K_s , we now turn to the charge sector. In Fig. 5, we present numerical results for the quantity $f(L)$ defined in Eq. (164), together with a fit to the functional form posited in Eq. (164). The spin Luttinger parameter is fixed as $K_s = 0.655$. The best-fit estimates are

$$\frac{\pi v_c}{8K_c} = 2.000, \quad (168)$$

and $b_2^c = 0.271$. The residuals are of order $\mathcal{O}(10^{-5})$.

Finally, in Fig. 6, we present numerical results for $\Delta E(0,0, \{m_\ell^s = 0, m_\ell^c = \delta_{\ell,1}\})$. Fitting the data to (163) with $K_s = 0.655$ results in estimates

$$v_c \approx 2.543, \quad (169)$$

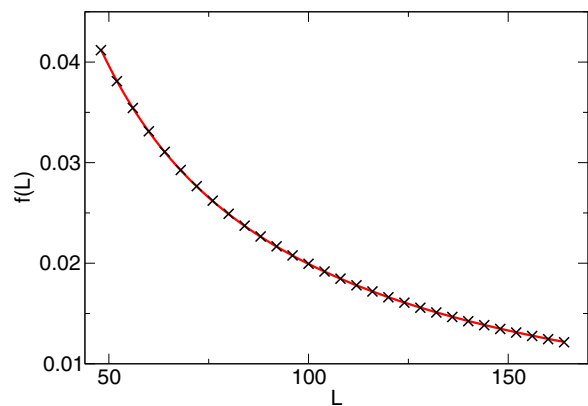


FIG. 5. (Color online) Crosses represent numerical results for $f(L)$ as defined in Eq. (164). The solid line is the best fit to (164) with $K_s = 0.655$.

and $\tilde{b}_2^c = -1.191$. Combining (168) and (169), we conclude that

$$K_c \approx 0.500. \quad (170)$$

F. Friedel oscillations

The analysis of finite-size energy levels presented above is clearly rather involved, and an independent check on the results for $K_{c,s}$ would clearly be very useful. Such a check is provided by analyzing Friedel oscillations of the charge density on a chain with open boundary conditions, cf Ref. [78]. We summarize the main steps of how to calculate the charge density for open boundary conditions in (perturbed) Luttinger liquid theory in Appendix D. For a quarter filled band, we obtain

$$n_j \approx \frac{1}{2} + \frac{d_1}{(D_j)^{2K_s}} + d_2 \frac{\sin\left[\left(\frac{\pi}{2} + \frac{p_1}{L+1}\right)j + p_2\right]}{(D_j)^{(K_c+K_s)/2}} + d_3 \frac{\cos\left[\left(\pi + \frac{2p_1}{L+1}\right)j + 2p_2\right]}{(D_j)^{2K_c}} + \dots, \quad (171)$$

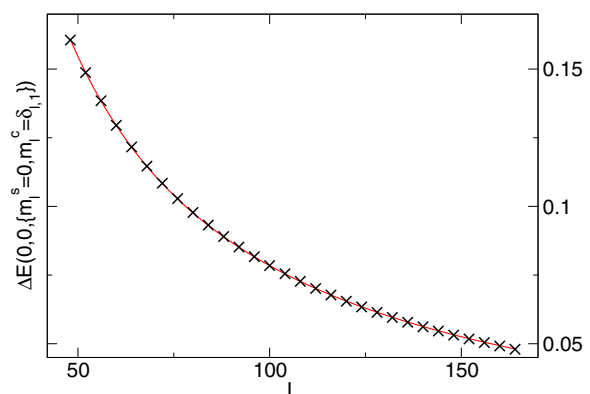


FIG. 6. (Color online) Crosses represent numerical results for $\Delta E(0,0, \{m_\ell^s = 0, m_\ell^c = \delta_{\ell,1}\})$. The solid line is the best fit to (163) for $K_s = 0.655$.

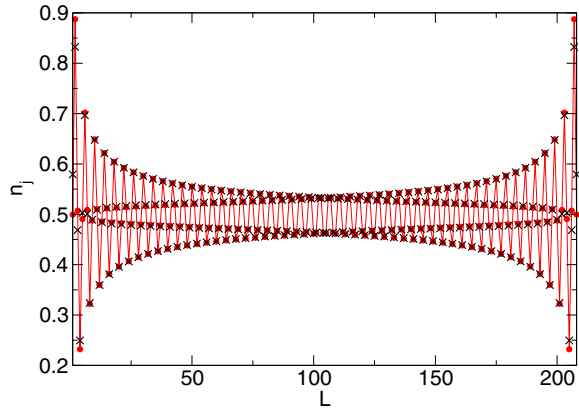


FIG. 7. (Color online) Crosses represent local density for a quarter filled band and $U = 3$, $V_1 = 0.85$, $V_2 = 1.1$, $J_1^z = 5.2$. The solid line is a fit to Eq. (171) with $K_s = 0.65$ and $K_c = 0.5$.

where D_j denotes

$$D_j = \frac{2(L+1)}{\pi} \sin\left(\frac{\pi j}{L+1}\right). \quad (172)$$

In Fig. 7, we compare the prediction (171) to DMRG results for a quarter filled band and system size $L = 208$. We fix the values of the Luttinger parameters to $K_s = 0.65$ and $K_c = 0.5$ and use the amplitudes d_j and phase shifts p_j as fit parameters. The agreement is very good except near the boundaries. The best fit is obtained for $d_1 = -0.05$, $d_2 = 0.83$, $d_3 = 0.01$, $p_1 = -\pi/4$, and $p_2 = -\pi/2$.

The good agreement between the expected behavior (171) and the DMRG results provides a consistency check on the values of $K_{c,s}$ extracted from the analysis of finite-size energy levels.

VIII. SUMMARY AND CONCLUSIONS

In this work, we have developed a new approach to deriving mobile impurity models for studying dynamical correlations in gapless models of spinful fermions. Our construction is based on the principle that our mobile impurity must carry the quantum numbers of a holon/antiholon (charge $\pm e$, spin 0) or a spinon (charge 0 and spin $\pm 1/2$). For the case of integrable models like the Hubbard chain, it is known from the exact solution that elementary excitations at finite energies are (anti)holons and spinons with precisely these quantum numbers. In integrable models these excitations are stable (i.e. do not decay). Breaking integrability is expected to render their lifetimes finite, but leaving their spin and charge quantum numbers intact.

To facilitate our construction, we first derived a representation of spinful nonlinear Luttinger liquids in terms of strongly interacting fermionic holons and spinons. At a particular *Luther-Emery* point for spin and charge, holons, and spinons become noninteracting. Using this as our point of reference, we derived a mobile impurity model appropriate for the description of threshold singularities in the single-particle spectral function for a general class of extended Hubbard models in their Luttinger liquid phase.

Our construction differs in important aspects from previous work by Schmidt, Imambekov, and Glazman [51,52]. However, we demonstrated explicitly how and why results for threshold exponents obtained in the two approaches coincide.

Finally, we presented a preliminary analysis of the question of how to realize, in the low-energy regime, the Luther-Emery point for spin and charge in a lattice model of interacting spinful fermions. We showed that the structure of allowed perturbations to the Luther-Emery point is such that fine tunings of various interactions is required. Achieving these fine tunings is very delicate, and we discussed in some detail what problems one encounters.

Our work raises a number of interesting questions that deserve further attention. First and foremost, further numerical studies are required in order to identify a parameter regime in an appropriate extended Hubbard model that, at least approximately, realizes the Luther-Emery point. Second, it would be very interesting to implement the numerical procedure we proposed for determining the parameters γ_α , $\bar{\gamma}_\alpha$ characterizing the threshold exponents. One first might want to reproduce the known exact results for the Hubbard model, before moving on to nonintegrable cases. Third, in close proximity to the Luther-Emery point, the mobile impurity model involves an additional marginal interaction that cannot be removed by a unitary transformation. It would be interesting to analyze its effects on the threshold exponents.

ACKNOWLEDGMENTS

This work was supported by the EPSRC under Grants EP/I032487/1 (FHLE) and EP/J014885/1 (FHLE), by the IRSES network QICFT (RGP and FHLE), the CNPq (RGP), and by the DFG under Grant SCHN 1169/2-1 (IS). We are grateful to Eric Jeckelmann for providing the DMRG code used in the numerical part of our analysis.

APPENDIX A: IRRELEVANT PERTURBATIONS TO THE LUTTINGER LIQUID HAMILTONIAN

One way of working out the allowed irrelevant perturbations to the Luttinger liquid Hamiltonian is by using symmetry considerations. Our starting point are extended Hubbard models of the kind (47). For the purposes of this appendix, we will assume all interactions to be *small*.

1. Symmetries

Our lattice models of interest are invariant under various symmetry operations. These symmetries are inherited by the bosonic low-energy description (52) and we now discuss their realizations.

a. Spin-flip symmetry

The lattice models of interest are invariant under exchange of up and down spins,

$$c_{j,\uparrow} \leftrightarrow c_{j,\downarrow}. \quad (A1)$$

It is realized at the level of the bosonic fields as

$$\begin{pmatrix} \varphi_s(x) \\ \bar{\varphi}_s(x) \\ \eta_\uparrow \\ \bar{\eta}_\uparrow \end{pmatrix} \rightarrow \begin{pmatrix} -\varphi_s(x) \\ -\bar{\varphi}_s(x) \\ \eta_\downarrow \\ \bar{\eta}_\downarrow \end{pmatrix}. \quad (\text{A2})$$

b. Translational invariance

The translation operator acts as

$$T^\dagger c_{j,\sigma} T = c_{j+1,\sigma}. \quad (\text{A3})$$

We can implement this on the level of bosonic fields by imposing the transformation properties

$$\begin{aligned} \begin{pmatrix} \varphi_c(x) \\ \bar{\varphi}_c(x) \end{pmatrix} &\rightarrow \begin{pmatrix} \varphi_c(x) - 2k_F a_0 \\ \bar{\varphi}_c(x) - 2k_F a_0 \end{pmatrix}, \\ \begin{pmatrix} \varphi_s(x) \\ \bar{\varphi}_s(x) \end{pmatrix} &\rightarrow \begin{pmatrix} \varphi_s(x) \\ \bar{\varphi}_s(x) \end{pmatrix}. \end{aligned} \quad (\text{A4})$$

We note that this transformation works for all higher harmonics in Eq. (48). Translational invariance of the Hamiltonian then implies that it generically may not contain any vertex operators of the charge boson. Exceptions to this rule occur at *commensurate fillings*

$$k_F a_0 = \pi \frac{p}{q}, \quad p, q \in \mathbb{N}. \quad (\text{A5})$$

Here operators of the form

$$\cos\left(\frac{q}{2}\Phi_c\right), \quad \sin\left(\frac{q}{2}\Phi_c\right) \quad (\text{A6})$$

are allowed to occur. As long as $q > 4$, such operators are highly irrelevant and do not play a role in the following discussion.

c. $U(1) \otimes U(1)$ Invariance

By this we mean that the Hamiltonian commutes with particle number and the z component of the total spin:

$$[H, \hat{S}^z] = [H, \hat{N}] = 0. \quad (\text{A7})$$

This symmetry implies that no vertex operators involving the dual fields Θ_c, Θ_s are allowed to occur in the expression for H .

d. Site parity

The reflection symmetry acts on the lattice fermion operators like

$$P c_{j,\sigma} P = c_{-j,\sigma}. \quad (\text{A8})$$

We see that P can be realized in the field theory as

$$\begin{aligned} P \varphi_a(x) P &= -\bar{\varphi}_a(-x), \quad P \bar{\varphi}_a(x) P = -\varphi_a(-x), \\ P \eta_\sigma P &= \bar{\eta}_\sigma. \end{aligned} \quad (\text{A9})$$

Crucially, parity acts on the unphysical Klein degrees of freedom as well. Moreover, we obtain the following constraints on the amplitudes $A_{n,m}$ in Eq. (48):

$$A_{n,m} = A_{1-n,-1-m}. \quad (\text{A10})$$

2. Dimension-two operators allowed by symmetry

We now list all the symmetry-allowed perturbations to the Luttinger liquid Hamiltonian for noninteracting spinful fermions with scaling dimensions 2, 3, and 4. Such perturbations will be of the form

$$\sum_j \hat{\Gamma}_j \lambda_j \int dx \mathcal{O}(x), \quad (\text{A11})$$

where λ_j are coupling constants and Γ_j are products of Klein factors. The only nontrivial combination of Klein factors allowed to appear is in fact

$$\eta_\uparrow \bar{\eta}_\uparrow \eta_\downarrow \bar{\eta}_\downarrow. \quad (\text{A12})$$

This is because all terms in our Hamiltonian (47) are of the form

$$c_{j,\sigma}^\dagger c_{k,\sigma}, \quad c_{j,\sigma}^\dagger c_{k,\tau} c_{l,\tau} c_{m,\sigma}. \quad (\text{A13})$$

Expressing the lattice fermion operators in terms of Bose fields by (48), and then imposing that for a given interaction to appear in the Hamiltonian it must not contain a rapidly oscillating factor $e^{ijk_F x}$, one finds that the Klein factors either cancel or combine to $\eta_\uparrow \bar{\eta}_\uparrow \eta_\downarrow \bar{\eta}_\downarrow$.

Taking this into account, we find five symmetry-allowed dimension-two operators:

$$\begin{aligned} \mathcal{O}_1^{(2)} &= \cos \Phi_s, \\ \mathcal{O}_2^{(2)} &= (\partial_x \varphi_s)^2 + (\partial_x \bar{\varphi}_s)^2, \\ \mathcal{O}_3^{(2)} &= \partial_x \varphi_s \partial_x \bar{\varphi}_s, \\ \mathcal{O}_4^{(2)} &= (\partial_x \varphi_c)^2 + (\partial_x \bar{\varphi}_c)^2, \\ \mathcal{O}_5^{(2)} &= \partial_x \varphi_c \partial_x \bar{\varphi}_c. \end{aligned} \quad (\text{A14})$$

We note that none of these lead to a coupling between spin and charge sectors. In order to see that the operator $\cos \Phi_s$ is allowed, but $\sin \Phi_s$ is not, one needs to consider the structure of Klein factors in Eq. (48).

3. Dimension-three operators allowed by symmetry

The analogous analysis for dimension-three operators gives the three possible perturbations involving only the charge sector:

$$\begin{aligned} \mathcal{O}_1^{(3)} &= (\partial_x \varphi_c)^3 + (\partial_x \bar{\varphi}_c)^3, \\ \mathcal{O}_2^{(3)} &= (\partial_x \varphi_c)^2 \partial_x \bar{\varphi}_c + (\partial_x \bar{\varphi}_c)^2 \partial_x \varphi_c, \\ \mathcal{O}_3^{(3)} &= \partial_x \varphi_c \partial_x^2 \bar{\varphi}_c - \partial_x \bar{\varphi}_c \partial_x^2 \varphi_c, \end{aligned} \quad (\text{A15})$$

and four possible perturbations that couple spin and charge sectors together:

$$\begin{aligned} \mathcal{O}_4^{(3)} &= (\partial_x \varphi_s)^2 \partial_x \varphi_c + (\partial_x \bar{\varphi}_s)^2 \partial_x \bar{\varphi}_c, \\ \mathcal{O}_5^{(3)} &= (\partial_x \varphi_s)^2 \partial_x \bar{\varphi}_c + (\partial_x \bar{\varphi}_s)^2 \partial_x \varphi_c, \\ \mathcal{O}_6^{(3)} &= \partial_x \varphi_s \partial_x \bar{\varphi}_s (\partial_x \bar{\varphi}_c + \partial_x \varphi_c), \\ \mathcal{O}_7^{(3)} &= (\partial_x \varphi_c + \partial_x \bar{\varphi}_c) \cos(\Phi_s). \end{aligned} \quad (\text{A16})$$

4. Dimension-four operators allowed by symmetry

Finally, we consider all symmetry-allowed dimension four operators.

a. Charge sector only

We find six perturbations involving only the charge sector:

$$\begin{aligned}
\mathcal{O}_1^{(4)} &= (\partial_x \varphi_c)^4 + (\partial_x \bar{\varphi}_c)^4, \\
\mathcal{O}_2^{(4)} &= (\partial_x \varphi_c)^2 (\partial_x \bar{\varphi}_c)^2, \\
\mathcal{O}_3^{(4)} &= (\partial_x \varphi_c)^3 \partial_x \bar{\varphi}_c + (\partial_x \bar{\varphi}_c)^3 \partial_x \varphi_c, \\
\mathcal{O}_4^{(4)} &= (\partial_x^2 \varphi_c)^2 + (\partial_x^2 \bar{\varphi}_c)^2, \\
\mathcal{O}_5^{(4)} &= \partial_x^2 \varphi_c \partial_x^2 \bar{\varphi}_c, \\
\mathcal{O}_6^{(4)} &= \partial_x^2 \varphi_c (\partial_x \bar{\varphi}_c)^2 - \partial_x^2 \bar{\varphi}_c (\partial_x \varphi_c)^2.
\end{aligned} \tag{A17}$$

Here we have used that

$$\begin{aligned}
&\partial_x^3 \varphi_c \partial_x \bar{\varphi}_c + \partial_x^3 \bar{\varphi}_c \partial_x \varphi_c \\
&= -2 \partial_x^2 \varphi_c \partial_x^2 \bar{\varphi}_c + \text{total derivative}.
\end{aligned} \tag{A18}$$

b. Spin sector only

We find altogether eight symmetry allowed perturbations involving only the spin sector:

$$\begin{aligned}
\mathcal{O}_7^{(4)} &= (\partial_x \varphi_s)^4 + (\partial_x \bar{\varphi}_s)^4, \\
\mathcal{O}_8^{(4)} &= (\partial_x \varphi_s)^2 (\partial_x \bar{\varphi}_s)^2, \\
\mathcal{O}_9^{(4)} &= (\partial_x \varphi_s)^3 \partial_x \bar{\varphi}_s + (\partial_x \bar{\varphi}_s)^3 \partial_x \varphi_s, \\
\mathcal{O}_{10}^{(4)} &= (\partial_x^2 \varphi_s)^2 + (\partial_x^2 \bar{\varphi}_s)^2, \\
\mathcal{O}_{11}^{(4)} &= \partial_x^2 \varphi_s \partial_x^2 \bar{\varphi}_s, \\
\mathcal{O}_{12}^{(4)} &= \cos(\Phi_s) \partial_x \varphi_s \partial_x \bar{\varphi}_s, \\
\mathcal{O}_{13}^{(4)} &= \cos(\Phi_s) [(\partial_x \varphi_s)^2 + (\partial_x \bar{\varphi}_s)^2].
\end{aligned} \tag{A19}$$

c. Terms coupling charge and spin

Finally, there are eight symmetry-allowed perturbations involving both spin and charge sectors:

$$\begin{aligned}
\mathcal{O}_{15}^{(4)} &= \cos(\Phi_s) \partial_x \varphi_c \partial_x \bar{\varphi}_c, \\
\mathcal{O}_{16}^{(4)} &= \cos(\Phi_s) [(\partial_x \varphi_c)^2 + (\partial_x \bar{\varphi}_c)^2], \\
\mathcal{O}_{17}^{(4)} &= [(\partial_x \varphi_s)^2 + (\partial_x \bar{\varphi}_s)^2] [(\partial_x \varphi_c)^2 + (\partial_x \bar{\varphi}_c)^2], \\
\mathcal{O}_{18}^{(4)} &= [(\partial_x \varphi_s)^2 + (\partial_x \bar{\varphi}_s)^2] \partial_x \varphi_c \partial_x \bar{\varphi}_c, \\
\mathcal{O}_{19}^{(4)} &= \partial_x \varphi_s \partial_x \bar{\varphi}_s [(\partial_x \varphi_c)^2 + (\partial_x \bar{\varphi}_c)^2], \\
\mathcal{O}_{20}^{(4)} &= \partial_x \varphi_s \partial_x \bar{\varphi}_s \partial_x \varphi_c \partial_x \bar{\varphi}_c, \\
\mathcal{O}_{21}^{(4)} &= [(\partial_x \varphi_s)^2 + (\partial_x \bar{\varphi}_s)^2] [\partial_x^2 \varphi_c - \partial_x^2 \bar{\varphi}_c], \\
\mathcal{O}_{22}^{(4)} &= \partial_x \varphi_s \partial_x \bar{\varphi}_s [\partial_x^2 \varphi_c - \partial_x^2 \bar{\varphi}_c].
\end{aligned} \tag{A20}$$

APPENDIX B: LIST OF IRRELEVANT OPERATORS AT THE LE POINT

The symmetries of the Hamiltonian at the Luther-Emery point are the same as those listed in Appendix A. Since at the

LE point all symmetry-allowed operators in the Hamiltonian are local in terms of free holons and spinons, we shall give the list of irrelevant operators directly in the fermionic representation. Among the operators listed in Appendix A, those that involve only derivatives of $\varphi_\alpha, \bar{\varphi}_\alpha$ preserve the same scaling dimension at the LE point; their expressions in the fermionic basis can be obtained straightforwardly by using bosonization identities for spinless fermions.

On the other hand, operators that contain $\cos(\Phi_s)$ require a more careful analysis. First, we note that, taking into account the Klein factors, the operator is actually represented by

$$\cos(\Phi_s) \rightarrow \eta_\uparrow \bar{\eta}_\downarrow \eta_\downarrow \bar{\eta}_\uparrow \cos(\Phi_s). \tag{B1}$$

Recall that spin flip and parity act nontrivially on $\eta_\sigma, \bar{\eta}_\sigma$. However, the product of four Majorana fermions in Eq. (B1) is invariant under both transformations. As a result, the Klein factors can be safely omitted in the symmetry analysis of the bosonized perturbations to the Luttinger model. At the LE point, however, $\cos(\Phi_s)$ must be refermionized into free spinons according to Eq. (67). In terms of spinon operators, spin-flip symmetry is equivalent to a particle-hole symmetry:

$$R_s \leftrightarrow R_s^\dagger, \quad L_s \leftrightarrow L_s^\dagger, \tag{B2}$$

while leaving the spinon Klein factors $\eta_s, \bar{\eta}_s$ invariant. Parity acts on spinon operators in the form

$$P R_s(x) P = L_s(-x), \quad P L_s(x) P = R_s(-x), \tag{B3}$$

$$P \eta_s P = \bar{\eta}_s, \quad P \bar{\eta}_s P = \eta_s. \tag{B4}$$

The refermionization of $\cos(\Phi_s)$ at the LE point yields

$$\begin{aligned}
\cos(\Phi_s) &\rightarrow \cos(\Phi_s^*/\sqrt{2}) \\
&\sim \pi (\eta_s R_s^\dagger \bar{\eta}_s L_s + \eta_s R_s \bar{\eta}_s L_s^\dagger) \\
&= -\pi (\eta_s \bar{\eta}_s R_s^\dagger L_s + \bar{\eta}_s \eta_s L_s^\dagger R_s).
\end{aligned} \tag{B5}$$

Notice that the operator in Eq. (B5) is invariant under the spin-flip transformation (B2) only if we take the spinon Klein factors into account explicitly. Nevertheless, in the following list of irrelevant operators, we shall omit the Klein factors for short and write simply

$$\cos(\Phi_s) \rightarrow (R_s^\dagger L_s + L_s^\dagger R_s). \tag{B6}$$

Since all the operators that stem from $\cos(\Phi_s)$ contain the same combination of Klein factors in Eq. (B5), we can adopt the prescription in Eq. (B6) supplemented by the *ad hoc* rule that spin-flip symmetry takes $R_s \rightarrow R_s^\dagger$ but $L_s \rightarrow -L_s^\dagger$.

Importantly, the operator $\cos(\Phi_s)$ has scaling dimension 2 at the SU(2)-symmetric weak coupling regime, but dimension 1 at the LE point. Therefore the scaling dimension of perturbations that contain $\cos(\Phi_s)$ is reduced by 1 as we go from weak coupling to the LE point. For instance, the marginal operator $\mathcal{O}_1^{(2)} = \cos(\Phi_s)$ at the SU(2) point becomes the relevant mass term of the Thirring model, $\cos(\Phi_s^*/\sqrt{2}) \sim R_s^\dagger L_s + L_s^\dagger R_s$ at the LE point, while the irrelevant (dimension-three) operator $\mathcal{O}_7^{(3)} = (\partial_x \bar{\varphi}_c + \partial_x \varphi_c) \cos(\Phi_s)$ at the SU(2) point gives rise to the marginal spin-charge coupling $(R_s^\dagger L_s + L_s^\dagger R_s)(R_c^\dagger R_c + L_c^\dagger L_c)$ at the LE point. This implies that, in order to have the complete list of irrelevant operators up to dimension four at the LE point, we have to consider the refermionization of

operators that have dimension 5 at the SU(2) point and were not included in the list in Appendix A. The latter correspond to operators $\mathcal{V}_{21}^{(4)}$ through $\mathcal{V}_{27}^{(4)}$ in the list below.

1. Dimension-three operators allowed by symmetry

$$\mathcal{V}_1^{(3)} = R_c^\dagger \partial_x^2 R_c + L_c^\dagger \partial_x^2 L_c + \text{H.c.}, \quad (\text{B7})$$

$$\mathcal{V}_2^{(3)} = R_c^\dagger R_c L_c^\dagger i \partial_x L_c - L_c^\dagger L_c R_c^\dagger i \partial_x R_c + \text{H.c.}, \quad (\text{B8})$$

$$\mathcal{V}_3^{(3)} = \partial_x (R_c^\dagger R_c) L_c^\dagger L_c - \partial_x (L_c^\dagger L_c) R_c^\dagger R_c, \quad (\text{B9})$$

$$\mathcal{V}_4^{(3)} = \partial_x R_s^\dagger \partial_x L_s + \partial_x L_s^\dagger \partial_x R_s, \quad (\text{B10})$$

$$\mathcal{V}_5^{(3)} = i R_s^\dagger \partial_x R_s L_s^\dagger R_s - i L_s^\dagger \partial_x L_s R_s^\dagger L_s + \text{H.c.}, \quad (\text{B11})$$

$$\mathcal{V}_6^{(3)} = R_c^\dagger R_c R_s^\dagger i \partial_x R_s - L_c^\dagger L_c L_s^\dagger i \partial_x L_s + \text{H.c.}, \quad (\text{B12})$$

$$\mathcal{V}_7^{(3)} = R_c^\dagger R_c L_s^\dagger i \partial_x L_s - L_c^\dagger L_c R_s^\dagger i \partial_x R_s + \text{H.c.}, \quad (\text{B13})$$

$$\mathcal{V}_9^{(3)} = \frac{\mathcal{V}_8^{(3)}}{i R_c^\dagger \partial_x R_c - i L_c^\dagger \partial_x L_c + \text{H.c.}} (R_c^\dagger R_c + L_c^\dagger L_c) R_s^\dagger R_s L_s^\dagger L_s + L_s^\dagger R_s, \quad (\text{B14})$$

$$(\text{B15})$$

$$\mathcal{V}_{10}^{(3)} = R_c^\dagger R_c L_c^\dagger L_c (R_s^\dagger L_s + L_s^\dagger R_s), \quad (\text{B16})$$

$$\mathcal{V}_{11}^{(3)} = \partial_x (R_c^\dagger R_c - L_c^\dagger L_c) (R_s^\dagger L_s + L_s^\dagger R_s). \quad (\text{B17})$$

2. Dimension-four operators allowed by symmetry

a. Charge sector only

$$\mathcal{V}_1^{(4)} = i R_c^\dagger \partial_x^3 R_c - i L_c^\dagger \partial_x^3 L_c + \text{H.c.}, \quad (\text{B18})$$

$$\mathcal{V}_2^{(4)} = R_c^\dagger \partial_x R_c L_c^\dagger \partial_x L_c + \text{H.c.}, \quad (\text{B19})$$

$$\mathcal{V}_3^{(4)} = R_c^\dagger \partial_x^2 R_c L_c^\dagger L_c + L_c^\dagger \partial_x^2 L_c R_c^\dagger R_c + \text{H.c.}, \quad (\text{B20})$$

$$\mathcal{V}_4^{(4)} = R_c^\dagger \partial_x R_c^\dagger R_c \partial_x R_c + L_c^\dagger \partial_x L_c^\dagger L_c \partial_x L_c, \quad (\text{B21})$$

$$\mathcal{V}_5^{(4)} = \partial_x (R_c^\dagger R_c) \partial_x (L_c^\dagger L_c), \quad (\text{B22})$$

$$\mathcal{V}_6^{(4)} = \partial_x (R_c^\dagger R_c) L_c^\dagger i \partial_x L_c + \partial_x (L_c^\dagger L_c) R_c^\dagger i \partial_x R_c + \text{H.c.} \quad (\text{B23})$$

b. Spin sector only

$$\mathcal{V}_7^{(4)} = i R_s^\dagger \partial_x^3 R_s - i L_s^\dagger \partial_x^3 L_s, \quad (\text{B24})$$

$$\mathcal{V}_8^{(4)} = R_s^\dagger \partial_x R_s L_s^\dagger \partial_x L_s + \text{H.c.}, \quad (\text{B25})$$

$$\mathcal{V}_9^{(4)} = R_s^\dagger \partial_x R_s^\dagger L_s \partial_x L_s + L_s^\dagger \partial_x L_s^\dagger R_s \partial_x R_s, \quad (\text{B26})$$

$$\mathcal{V}_{10}^{(4)} = R_s^\dagger \partial_x^2 R_s L_s^\dagger L_s + L_s^\dagger \partial_x^2 L_s R_s^\dagger R_s + \text{H.c.}, \quad (\text{B27})$$

$$\mathcal{V}_{11}^{(4)} = R_s^\dagger \partial_x R_s^\dagger R_s \partial_x R_s + L_s^\dagger \partial_x L_s^\dagger L_s \partial_x L_s, \quad (\text{B28})$$

$$\mathcal{V}_{12}^{(4)} = \partial_x (R_s^\dagger R_s) \partial_x (L_s^\dagger L_s). \quad (\text{B29})$$

c. Terms coupling charge and spin

$$\mathcal{V}_{13}^{(4)} = (i R_c^\dagger \partial_x R_c + \text{H.c.}) (i R_s^\dagger \partial_x R_s + \text{H.c.}) + (i L_c^\dagger \partial_x L_c + \text{H.c.}) (i L_s^\dagger \partial_x L_s + \text{H.c.}), \quad (\text{B30})$$

$$\mathcal{V}_{14}^{(4)} = (i R_c^\dagger \partial_x R_c + \text{H.c.}) (i L_s^\dagger \partial_x L_s + \text{H.c.}) + (i L_c^\dagger \partial_x L_c + \text{H.c.}) (i R_s^\dagger \partial_x R_s + \text{H.c.}), \quad (\text{B31})$$

$$\mathcal{V}_{15}^{(4)} = R_c^\dagger R_c L_c^\dagger L_c (i R_s^\dagger \partial_x R_s - i L_s^\dagger \partial_x L_s + \text{H.c.}), \quad (\text{B32})$$

$$\mathcal{V}_{16}^{(4)} = (i R_c^\dagger \partial_x R_c - i L_c^\dagger \partial_x L_c + \text{H.c.}) R_s^\dagger R_s L_s^\dagger L_s, \quad (\text{B33})$$

$$\mathcal{V}_{17}^{(4)} = R_c^\dagger R_c L_c^\dagger L_c R_s^\dagger R_s L_s^\dagger L_s, \quad (\text{B34})$$

$$\mathcal{V}_{18}^{(4)} = \partial_x (R_c^\dagger R_c) (i R_s^\dagger \partial_x R_s + \text{H.c.}) + \partial_x (L_c^\dagger L_c) (i L_s^\dagger \partial_x L_s + \text{H.c.}), \quad (\text{B35})$$

$$\mathcal{V}_{19}^{(4)} = \partial_x (R_c^\dagger R_c) (i L_s^\dagger \partial_x L_s + \text{H.c.}) + \partial_x (L_c^\dagger L_c) (i R_s^\dagger \partial_x R_s + \text{H.c.}), \quad (\text{B36})$$

$$\mathcal{V}_{20}^{(4)} = \partial_x (R_c^\dagger R_c - L_c^\dagger L_c) R_s^\dagger R_s L_s^\dagger L_s, \quad (\text{B37})$$

$$\mathcal{V}_{21}^{(4)} = (R_c^\dagger \partial_x^2 R_c + L_c^\dagger \partial_x^2 L_c + \text{H.c.}) (R_s^\dagger L_s + L_s^\dagger R_s), \quad (\text{B38})$$

$$\mathcal{V}_{22}^{(4)} = (R_c^\dagger R_c L_c^\dagger i \partial_x L_c - L_c^\dagger L_c R_c^\dagger i \partial_x R_c + \text{H.c.}) \times (R_s^\dagger L_s + L_s^\dagger R_s), \quad (\text{B39})$$

$$\mathcal{V}_{23}^{(4)} = R_c^\dagger R_c R_s^\dagger i \partial_x R_s L_s^\dagger R_s - L_c^\dagger L_c L_s^\dagger i \partial_x L_s R_s^\dagger L_s + \text{H.c.}, \quad (\text{B40})$$

$$\mathcal{V}_{24}^{(4)} = R_c^\dagger R_c L_s^\dagger i \partial_x L_s R_s^\dagger L_s - L_c^\dagger L_c R_s^\dagger i \partial_x R_s L_s^\dagger R_s + \text{H.c.}, \quad (\text{B41})$$

$$\mathcal{V}_{25}^{(4)} = \partial_x^2 (R_c^\dagger R_c + L_c^\dagger L_c) (R_s^\dagger L_s + L_s^\dagger R_s), \quad (\text{B42})$$

$$\mathcal{V}_{26}^{(4)} = \partial_x (R_c^\dagger i \partial_x R_c + L_c^\dagger i \partial_x L_c) (R_s^\dagger L_s + L_s^\dagger R_s), \quad (\text{B43})$$

$$\mathcal{V}_{27}^{(4)} = [\partial_x (R_c^\dagger R_c) L_c^\dagger L_c - \partial_x (L_c^\dagger L_c) R_c^\dagger R_c] (R_s^\dagger L_s + L_s^\dagger R_s). \quad (\text{B44})$$

APPENDIX C: CONSTRAINING THE MOBILE IMPURITY MODEL IN THE SU(2)-SYMMETRIC CASE

We can impose SU(2) symmetry in the parameters of the mobile impurity model of Sec. V by requiring that the edge exponents of longitudinal and transverse spin-spin correlations coincide [43]. First, consider the longitudinal component of the spin density operator:

$$S^z(x) \sim R_\uparrow^\dagger(x) R_\uparrow(x) - R_\downarrow^\dagger(x) R_\downarrow(x) \sim \mathcal{O}_s^\dagger(x) \mathcal{O}_s(x), \quad (\text{C1})$$

where the charge strings are canceled in the sense of the lowest order in the OPE. We then project $\mathcal{O}_s(x)$ so as to create a high-energy spinon:

$$\mathcal{O}_s(x) \sim e^{-iqx} \chi_s^\dagger(x) e^{\frac{i}{\sqrt{2}} \Phi_s^*(x)}, \quad (\text{C2})$$

while $\mathcal{O}_s^\dagger(x)$ acts only in the low-energy subband:

$$\mathcal{O}_s^\dagger(x) \sim e^{\frac{i}{\sqrt{2}} \Phi_s^* - \frac{i}{\sqrt{2}} \Phi_s(x)}. \quad (\text{C3})$$

Cancelling the neutral string, we obtain

$$S^z(x) \sim e^{-iqx} \chi_s^\dagger(x) e^{\frac{i}{\sqrt{2}} \Phi_s^*(x)}. \quad (\text{C4})$$

In terms of the transformed impurity field

$$S^z(x) \sim e^{-iqx} a_s^\dagger(x) e^{i(\frac{1}{\sqrt{2}} + \gamma_s) \Phi_s^* + i\gamma_s \bar{\Phi}_s^* + i\gamma_c \Phi_c^* + i\gamma_c \bar{\Phi}_c^*}. \quad (\text{C5})$$

Now, consider the transverse component:

$$\begin{aligned} S^-(x) &\sim R_{\downarrow}^{\dagger}(x)R_{\uparrow}(x) \\ &\sim \mathcal{O}_s(x)\mathcal{O}_s(x) \\ &\sim e^{-iqx}\chi_s^{\dagger}(x)e^{-\frac{i}{2\sqrt{2}}\varphi_s^*(x)+\frac{i}{2\sqrt{2}}\bar{\varphi}_s^*(x)} \\ &= e^{-iqx}d_s^{\dagger}(x)e^{-i(\frac{1}{2\sqrt{2}}-\gamma_s)\varphi_s^*+i(\frac{1}{2\sqrt{2}}+\bar{\gamma}_s)\varphi_s^*}e^{i\gamma_c\varphi_c^*+i\bar{\gamma}_c\bar{\varphi}_c^*}. \end{aligned} \quad (\text{C6})$$

Given the expressions (C5) and (C6) we can calculate threshold exponents in the Fourier transforms of the spin correlations functions $\langle S^z(x,t)S^z(0,0) \rangle$ and $\langle S^+(x,t)S^-(0,0) \rangle$ and impose that they share the same exponents in the SU(2)-symmetric case. This has to be the case even for higher harmonics, taking into account backscattering processes [43]. A shortcut is to compare the scaling dimensions of the strings in Eqs. (C5) and (C6). We must have

$$\frac{1}{\sqrt{2}} + \gamma_s = \frac{1}{2\sqrt{2}} - \gamma_s, \quad (\text{C7})$$

$$-\bar{\gamma}_s = \frac{1}{2\sqrt{2}} + \bar{\gamma}_s. \quad (\text{C8})$$

It follows that SU(2) symmetry imposes

$$\gamma_s = \bar{\gamma}_s = -\frac{1}{4\sqrt{2}}. \quad (\text{C9})$$

These values of $\gamma_s, \bar{\gamma}_s$ are of order 1, as expected since the spinons are strongly interacting at the SU(2) point. Moreover, these values are consistent with the exact result for the Hubbard model at zero magnetic field (see Sec. VB). Using Eq. (C9) and setting $K_s = 1$ in Eq. (110) yields

$$\nu_{s,+} = \nu_{s,-} = 0. \quad (\text{C10})$$

APPENDIX D: FRIEDEL OSCILLATIONS

In this Appendix, we summarize some useful facts regarding Friedel oscillations for open boundary conditions. At low energies, the charge density operator has an expansion of the form

$$n_j \sim \sum_{n=0} \rho_{2nk_F}(x), \quad (\text{D1})$$

where $\rho_{2nk_F}(x)$ denotes the Fourier components with momenta $\pm 2nk_F$. For periodic boundary conditions it follows from (48) and the site-parity symmetry (A9) that the leading contributions to the $2k_F$ and $4k_F$ components are

$$\begin{aligned} \rho_{2k_F}(x) &= \widehat{A}_{2k_F} \sin\left(\frac{\Phi_c}{2} - 2k_F x\right) \cos\left(\frac{\Phi_s}{2}\right) + \dots, \\ \rho_{4k_F}(x) &= \widehat{A}_{4k_F} \cos(\Phi_c - 4k_F x) + \dots, \end{aligned} \quad (\text{D2})$$

where \widehat{A}_{2k_F} and \widehat{A}_{4k_F} are nonuniversal amplitudes that include Klein factors. The leading contributions to zero-momentum component are

$$\rho_0(x) = n - \frac{1}{2\pi} \partial_x \Phi_c + \widehat{A}_0 \partial_x \Phi_c \cos\left(\frac{\Phi_s}{2}\right) + \dots, \quad (\text{D3})$$

where n is the band filling.

1. Open boundary conditions

For open boundary conditions we still have expansions like (48), but the chiral Bose fields no longer commute and hence the Klein factors $\Gamma_{n,m}^{\sigma}$ need to be adjusted accordingly. The mode expansions for the chiral Bose fields are

$$\begin{aligned} \varphi_c(x) &= \frac{a + \pi_0}{2} + \frac{x\varphi_0}{2(L+1)} + i \sum_{n=1}^{\infty} \sqrt{\frac{2}{n}} (e^{-iq_n x} \alpha_n - \text{H.c.}), \\ \bar{\varphi}_c(x) &= \frac{a - \pi_0}{2} + \frac{x\varphi_0}{2(L+1)} - i \sum_{n=1}^{\infty} \sqrt{\frac{2}{n}} (e^{iq_n x} \alpha_n - \text{H.c.}), \end{aligned} \quad (\text{D4})$$

where $[\pi_0, \varphi_0] = 8\pi i$ and $q_n = \pi n/(L+1)$. The commutator between different chiralities is

$$[\varphi_{\alpha}(x), \bar{\varphi}_{\alpha}(y)] = \begin{cases} 0 & \text{if } x = y = 0, \\ 2\pi i & \text{if } 0 < x, y < L+1, \\ 4\pi i & \text{if } x = y = L+1. \end{cases} \quad (\text{D5})$$

The boundary conditions on the Fermi creation and annihilation operators are

$$c_{j=0,\sigma} = 0 = c_{j=L+1,\sigma}. \quad (\text{D6})$$

Imposing the boundary conditions (D6) on the bosonized expression (48) [with Klein factors appropriate for the mode expansions (D4)] leads to conditions of the form

$$\begin{aligned} \Phi_c(0)|\psi_0\rangle &= c_1|\psi_0\rangle, & \Phi_c(L+1)|\psi_0\rangle &= c_2|\psi_0\rangle, \\ \Phi_s(0)|\psi_0\rangle &= \Phi_s(L+1)|\psi_0\rangle &= c'_1|\psi_0\rangle. \end{aligned} \quad (\text{D7})$$

Importantly, the actual values of the $c_{1,2}$ and $c'_{1,2}$ depend on all the amplitudes $A_{n,m}$ in Eq. (48) and are thus nonuniversal.

2. Friedel oscillations

For open boundary conditions, the $2k_F$ and $4k_F$ components of the total charge density are again given by expressions of the form (D2). Using the mode expansions, we then can determine the form of the Friedel oscillations

$$\begin{aligned} \langle \psi_0 | \rho_{2k_F}(x) | \psi_0 \rangle &\sim B_{2k_F} \frac{\sin(2k'_F x - \frac{c_1}{2})}{\left(\frac{2}{\epsilon} \sin\left(\frac{\pi x}{L+1}\right)\right)^{(1+K_c)/2}}, \\ \langle \psi_0 | \rho_{4k_F}(x) | \psi_0 \rangle &\sim B_{4k_F} \frac{\cos(4k'_F x - c_1)}{\left(\frac{2}{\epsilon} \sin\left(\frac{\pi x}{L+1}\right)\right)^{2K_c}}, \end{aligned} \quad (\text{D8})$$

where ϵ is a short-distance cutoff, we have taken into account $K_c \neq 1$ and defined

$$k'_F = k_F + \frac{c_1 - c_2}{4(L+1)}. \quad (\text{D9})$$

The upshot is that Friedel oscillations involve two *nonuniversal* interaction-dependent parameters: the phase shift c_1 and the $1/L$ shift of k_F .

- [1] C. Xu and S. Sachdev, *Phys. Rev. Lett.* **105**, 057201 (2010).
- [2] V. V. Deshpande, M. Bockrath, L. I. Glazman, and A. Yacoby, *Nature (London)* **464**, 209 (2010).
- [3] O. M. Auslaender *et al.*, *Science* **295**, 825 (2002).
- [4] B. J. Kim *et al.*, *Nat. Phys.* **2**, 397 (2006).
- [5] Y. Jompol *et al.*, *Science* **325**, 597 (2009).
- [6] J. Schlappa *et al.*, *Nature (London)* **485**, 82 (2012).
- [7] F. H. L. Essler, H. Frahm, F. Göhmann, A. Klümper, and V. E. Korepin, *The One Dimensional Hubbard Model* (Cambridge University Press, Cambridge, 2005).
- [8] F. H. L. Essler and V. E. Korepin, *Phys. Rev. Lett.* **72**, 908 (1994).
- [9] F. H. L. Essler and V. E. Korepin, *Nucl. Phys. B* **426**, 505 (1994).
- [10] N. Andrei, [arXiv:cond-mat/9408101](https://arxiv.org/abs/cond-mat/9408101).
- [11] T. Deguchi, F. H. L. Essler, F. Göhmann, V. E. Korepin, A. Klümper, and K. Kusakabe, *Phys. Rep.* **331**, 197 (2000).
- [12] K. Penc, F. Mila, and H. Shiba, *Phys. Rev. Lett.* **75**, 894 (1995).
- [13] J. Favand, S. Haas, K. Penc, F. Mila, and E. Dagotto, *Phys. Rev. B* **55**, R4859 (1997).
- [14] K. Penc, K. Hallberg, F. Mila, and H. Shiba, *Phys. Rev. B* **55**, 15475 (1997).
- [15] H. Benthien, F. Gebhard, and E. Jeckelmann, *Phys. Rev. Lett.* **92**, 256401 (2004).
- [16] A. E. Feiguin and D. A. Huse, *Phys. Rev. B* **79**, 100507(R) (2009).
- [17] M. Arikawa, Y. Saiga, and Y. Kuramoto, *Phys. Rev. Lett.* **86**, 3096 (2001).
- [18] M. Arikawa, T. Yamamoto, Y. Saiga, and Y. Kuramoto, *Nucl. Phys. B* **702**, 380 (2004).
- [19] A. B. Zamolodchikov and Al. B. Zamolodchikov, *Ann. Phys.* **120**, 253 (1979).
- [20] L. D. Faddeev, *Sov. Sci. Rev. Math. Phys. C* **1**, 107 (1980).
- [21] R. A. J. van Elburg and K. Schoutens, *Phys. Rev. B* **58**, 15704 (1998).
- [22] G. I. Japaridze, A. A. Nersesyan, and P. B. Wiegmann, *Nucl. Phys. B* **230**, 511 (1984).
- [23] F. Woynarovich, *J. Phys. A* **22**, 4243 (1989).
- [24] H. Frahm and V. E. Korepin, *Phys. Rev. B* **42**, 10553 (1990).
- [25] I. Affleck, in *Fields, Strings and Critical Phenomena*, edited by E. Brézin and J. Zinn-Justin, (Elsevier, Amsterdam, 1989).
- [26] A. O. Gogolin, A. A. Nersesyan, and A. M. Tsvelik, *Bosonization and Strongly Correlated Systems* (Cambridge University Press, Cambridge, 1999).
- [27] T. Giamarchi, *Quantum Physics in One Dimension* (Clarendon Press, Oxford, 2004).
- [28] M. Pustilnik, M. Khodas, A. Kamenev, and L. I. Glazman, *Phys. Rev. Lett.* **96**, 196405 (2006).
- [29] A. Rozhkov, *Eur. Phys. J. B* **47**, 193 (2005).
- [30] A. V. Rozhkov, *Phys. Rev. B* **74**, 245123 (2006).
- [31] J. M. P. Carmelo, K. Penc, L. M. Martelo, P. D. Sacramento, J. M. B. Lopes, Dos Santos, R. Claessen, M. Sing, and U. Schwingenschlögl, *Europhys. Lett.* **67**, 233 (2004).
- [32] J. M. P. Carmelo, K. Penc, P. D. Sacramento, M. Sing, and R. Claessen, *J. Phys.: Condens. Matter* **18**, 5191 (2006).
- [33] J. M. P. Carmelo, D. Bozi, and K. Penc, *J. Phys. Cond. Mat.* **20**, 415103 (2008).
- [34] R. G. Pereira, J. Sirker, J.-S. Caux, R. Hagemans, J. M. Maillet, S. R. White, and I. Affleck, *Phys. Rev. Lett.* **96**, 257202 (2006).
- [35] E. Bettelheim, A. G. Abanov, and P. Wiegmann, *Phys. Rev. Lett.* **97**, 246401 (2006).
- [36] M. Khodas, M. Pustilnik, A. Kamenev, and L. I. Glazman, *Phys. Rev. Lett.* **99**, 110405 (2007).
- [37] M. Khodas, M. Pustilnik, A. Kamenev, and L. I. Glazman, *Phys. Rev. B* **76**, 155402 (2007).
- [38] R. G. Pereira, S. R. White, and I. Affleck, *Phys. Rev. Lett.* **100**, 027206 (2008).
- [39] A. Imambekov and L. I. Glazman, *Phys. Rev. Lett.* **100**, 206805 (2008).
- [40] V. V. Cheianov and M. Pustilnik, *Phys. Rev. Lett.* **100**, 126403 (2008).
- [41] E. Bettelheim, A. G. Abanov, and P. Wiegmann, *J. Phys. A* **41**, 392003 (2008).
- [42] A. G. Abanov, E. Bettelheim, and P. Wiegmann, *J. Phys. A* **42**, 135201 (2009).
- [43] A. Imambekov and L. I. Glazman, *Phys. Rev. Lett.* **102**, 126405 (2009).
- [44] A. Imambekov and L. I. Glazman, *Science* **323**, 228 (2009).
- [45] R. G. Pereira, S. R. White, and I. Affleck, *Phys. Rev. B* **79**, 165113 (2009).
- [46] R. G. Pereira, *Int. J. Mod. Phys. B* **26**, 1244008 (2012).
- [47] A. V. Rozhkov, *Phys. Rev. Lett.* **112**, 106403 (2014).
- [48] T. Price and A. Lamacraft, *Phys. Rev. B* **90**, 241415 (2014).
- [49] R. G. Pereira and E. Sela, *Phys. Rev. B* **82**, 115324 (2010).
- [50] R. G. Pereira, K. Penc, S. R. White, P. D. Sacramento, and J. M. P. Carmelo, *Phys. Rev. B* **85**, 165132 (2012).
- [51] T. L. Schmidt, A. Imambekov, and L. I. Glazman, *Phys. Rev. Lett.* **104**, 116403 (2010).
- [52] T. L. Schmidt, A. Imambekov, and L. I. Glazman, *Phys. Rev. B* **82**, 245104 (2010).
- [53] F. H. L. Essler, *Phys. Rev. B* **81**, 205120 (2010).
- [54] A. Imambekov, T. L. Schmidt, and L. I. Glazman, *Rev. Mod. Phys.* **84**, 1253 (2012).
- [55] O. Tsypliyatyev and A. J. Schofield, *Phys. Rev. B* **90**, 014309 (2014).
- [56] L. Seabra, F. H. L. Essler, F. Pollmann, I. Schneider, and T. Veness, *Phys. Rev. B* **90**, 245127 (2014).
- [57] V. E. Korepin, N. M. Bogoliubov, and A. G. Izergin, *Quantum Inverse Scattering Method and Correlation Functions* (Cambridge University Press, Cambridge, 1999).
- [58] L. D. Faddeev and L. Takhtajan, *Jour. Sov. Math.* **24**, 241 (1984).
- [59] F. H. L. Essler and R. M. Konik, in *From Fields to Strings: Circumnavigating Theoretical Physics*, ed. M. Shifman, A. Vainshtein, and J. Wheeler (World Scientific, Singapore, 2005); and references therein; [arXiv:cond-mat/0412421](https://arxiv.org/abs/cond-mat/0412421).
- [60] K. D. Schotte and U. Schotte, *Phys. Rev.* **182**, 479 (1969).
- [61] A. Luther and V. J. Emery, *Phys. Rev. Lett.* **33**, 589 (1974).
- [62] F. D. M. Haldane, *Phys. Rev. Lett.* **47**, 1840 (1981).
- [63] H. Frahm and V. E. Korepin, *Phys. Rev. B* **43**, 5653 (1991).
- [64] D. B. Abraham, F. H. L. Essler, and A. Maciolek, *Phys. Rev. Lett.* **98**, 170602 (2007).
- [65] S. Coleman, *Phys. Rev. D* **11**, 2088 (1975).
- [66] M. B. Zvonarev, V. V. Cheianov, and T. Giamarchi, *J. Stat. Mech.* (2009) P07035.
- [67] H. Karimi and I. Affleck, *Phys. Rev. B* **84**, 174420 (2011).
- [68] C. G. Callan, I. R. Klebanov, A. W. W. Ludwig, and J. M. Maldacena, *Nucl. Phys. B* **422**, 417 (1994).
- [69] T. Xiang, *Phys. Rev. B* **53**, R10445(R) (1996).
- [70] U. Schollwöck, *Rev. Mod. Phys.* **77**, 259 (2005).
- [71] F. H. L. Essler, V. E. Korepin, and K. Schoutens, *Phys. Rev. Lett.* **67**, 3848 (1991).

- [72] F. H. L. Essler, V. E. Korepin, and K. Schoutens, *Nucl. Phys. B* **372**, 559 (1992).
- [73] M. Ogata and H. Shiba, *Phys. Rev. B* **41**, 2326 (1990).
- [74] S. Eggert, *Phys. Rev. B* **54**, R9612 (1996).
- [75] K. Okamoto and K. Nomura, *Phys. Lett. A* **169**, 433 (1992).
- [76] S. R. White, *Phys. Rev. Lett.* **69**, 2863 (1992).
- [77] S. R. White, *Phys. Rev. B* **48**, 10345 (1993).
- [78] S. A. Söfing, M. Bortz, I. Schneider, A. Struck, M. Fleischhauer, and S. Eggert, *Phys. Rev. B* **79**, 195114 (2009).